AMERICAN MUSEUM NOVITATES

Number 3727, 58 pp. November 21, 2011

Redescription of a Nearly Complete Skull of *Plateosaurus* (Dinosauria: Sauropodomorpha) from the Late Triassic of Trossingen (Germany)

ALBERT PRIETO-MÁRQUEZ[1] AND MARK A. NORELL[2]

ABSTRACT

The nearly complete, disarticulated skull of AMNH FARB 6810, a specimen of the basal sauropodomorph *Plateosaurus* collected in 1925 from the Norian (Late Triassic) strata of the Knollenmergel beds of Trossingen (Germany), is redescribed. This study supports referral of AMNH FARB 6810 to *P. erlenbergiensis* on the basis of the following characters: occipital condyle above level of parasphenoid; basisphenoid with transverse, subvertical lamina extending between basipterygoid processes, with ventrally projecting median process; and peglike process projecting medially from the middle of the palatine. Furthermore, *P. longiceps* is regarded a junior synonym of *P. erlenbergiensis* because the type specimen of the latter is diagnostic (displaying the above-noted apomorphies of the braincase and palatine) and, chronologically, *P. erlenbergiensis* has priority over *P. longiceps*.

INTRODUCTION

Sauropodomorphs were moderate-sized (4–6 m) to gigantic (over 30 m in length) herbivorous saurischian dinosaurs, including the sauropods characterized by columnar limbs, bulky torsos, and long necks ending in relatively small skulls (Wilson and Curry Rogers, 2005). These animals were one of the most diverse and abundant clades of Mesozoic terrestrial herbivores and

[1] Division of Paleontology, American Museum of Natural History. Current address: Bayerische Staatssammlung für Paläontologie und Geologie, Richard-Wagner-Straße 10, D-80333 Munich, Germany.
[2] Division of Paleontology, American Museum of Natural History.

 ISSN 0003-0082

represent one of the three major radiations of dinosaurs (Sereno, 1999). According to a few authors, the basal sauropodomorphs are monophyletic, the Prosauropoda, that is phylogenetically positioned as the sister clade to sauropods (Cruickshank, 1975; Sereno, 1989; Galton, 1990; Gauffre, 1995; Wilson and Sereno, 1998; Galton and Upchurch, 2004; Barrett et al., 2005; Martínez, 2009). However, most studies have questioned prosauropod monophyly and most currently agree that these animals form a paraphyletic assemblage of successive outgroup taxa to Sauropoda (Romer, 1956; Colbert, 1964; Charig et al., 1965; Bonaparte, 1969; 1999; Yates, 2003a; 2004; Yates and Kitching, 2003; Upchurch et al., 2007; Martínez and Alcober, 2009; Yates et al., 2010; Novas et al., 2011; Pol et al., 2011). Basal sauropodomorphs (although not monophyletic) are among the earliest and more primitive dinosaurs, with a fossil record that spans the Carnian (Early Late Triassic) through the Early Jurassic (Galton and Upchurch, 2004). Their fossil remains have so far been recovered in Europe (Galton, 1973; 1986; 2000; Yates, 2003b), Africa (Barrett, 2004; 2009; Sues et al., 2004; Yates et al., 2010), Asia (Young, 1941a, 1941b; 1942; Bai et al., 1990; Zhang and Yang, 1994), both Americas (Galton, 1976; Bonaparte, 1978; Attridge et al., 1985; Martínez, 1999; 2009; Sertich and Loewen, 2010), and Antarctica (Smith and Pol, 2007).

The best-represented basal sauropodomorph, as well as the Triassic dinosaur with the richest fossil record and one of the better-known early dinosaurs, is *Plateosaurus*. This genus occurs in Norian (Late Triassic) strata of Germany, Switzerland, Norway, Greenland, and France (Weishampel and Chapman, 1990; Jenkins et al., 1995; Galton and Upchurch, 2004). Its type species, *P. engelhardti*, was one of the first dinosaurs to be scientifically recognized and named (Meyer, 1837). However, the better-known species is *P. longiceps* (Jaekel, 1913–1914; see also Galton, 2000, 2001), here regarded a junior synonym of *P. erlenbergiensis* (see Discussion and conclusion). This species is represented by abundant material that includes complete skeletons and skulls and is often found as mass accumulations in bonebeds (Sander, 1992; Klein, 2004). This great quality and quantity of material has made *P. erlenbergiensis* a good model for studies seeking to understand the paleobiology and evolution of early saurischian dinosaurs, including research on the taphonomy (Sander, 1992; Sander and Klein, 2005) anatomy (Galton, 1984; 1985; 1997), systematics (Yates, 2003b), and functional morphology (Gunga et al., 2007; Mallison, 2010a, 2010b) of this species.

Among the fossil materials of *Plateosaurus*, there is one specimen, AMNH FARB 6810, that is key for a more comprehensive understanding of the anatomy of this taxon. The specimen was collected in 1925 by Friedrich von Huene from Norian strata of the Knollenmergel Formation (Trossingen, southern Germany). AMNH FARB 6810 consists of a complete skeleton found in articulation that includes a well-preserved and nearly complete skull. This skull is important because most of its individual elements have been disarticulated by careful preparation and because of its excellent preservation, which allows for detailed three-dimensional documentation of the cranial osteology of *Plateosaurus*. Specifically, the skull of AMNH FARB 6810 preserves the left and right mandibles (including dentary, surangular, angular, coronoid, splenial, prearticular, and articular), the left and right premaxillae, maxillae, nasals, prefrontals, lacrimals, postorbitals, jugals, quadratojugals, quadrates, squamosals, partial palate (pterygoids, palatines, ectopterygoids, epipterygoids, and vomers), and neurocranial elements (frontals,

TABLE 1. Selected measurements (mm) of facial elements of the skull of AMNH FARB 6810

Skull (articulated)	
Total length (rostral tip of premaxilla to posterior end of articular)	330.0
Height (dorsal margin of supratemporal fenestra to ventral margin of angular)	126.5
Premaxilla (left)	
Length (anterior margin to distal tip of ventral process)	81.9
Length of alveolar margin	38.7
Maxilla (left)	
Maximum length	179.4
Height (dorsal tip of dorsal process to alveolar margin)	81.2
Prefrontal (left)	
Maximum length of dorsomedial flange	69.6
Height (dorsal margin to distal tip of ventral ramus, following axis of ventral ramus)	58.4
Lacrimal (left)	
Height (dorsal margin to ventral border of finlike process)	77.3
Maximum length of dorsal region	59.0
Postorbital (right)	
Maximum length (along anterior and posterior rami)	81.4
Height (inflected point of dorsal margin to distal tip of ventral ramus)	51.6
Squamosal (right)	
Length (along dorsal region)	57.3
Height (dorsal margin to distal tip of quadrate ramus)	60.4
Jugal (right)	
Length (between tips of anterior and posterior rami)	102.7
Height (along bisecting axis of dorsal ramus)	49.1
Quadratojugal (left)	
Maximum length (along anteroventral margin)	71.0
Length (end of anterior ramus to end of ventral ramus)	38.3
Quadrate (left)	
Maximum height	94.1
Maximum width of pterygoid flange	31.0

parietal, and nearly complete braincase). Galton (1984, 1985) featured AMNH FARB 6810 in his descriptions of the cranial anatomy of *Plateosaurus,* along with other materials recovered from various Norian localities in Germany. However, Galton's description of AMNH FARB 6810 focused more on the articular relationships among the different elements of the skull than on the geometry and morphological attributes of each individual bone. In the 25 years since Galton's early work, numerous basal sauropodomorph species have been discovered and named (Galton and Upchurch, 2004; Smith and Pol, 2007; Martínez, 2009; Barrett, 2009; Yates et al.,

TABLE 2. Selected measurements (mm) of palatal elements of the skull of AMNH FARB 6810.

Pterygoid (right)	
Maximum length (rostral tip of anterior ramus to distal end of dorsal process of quadrate ramus)	142.4
Height (distal end of dorsal process of quadrate ramus to posterior border of ventral flange)	95.1
Epipterygoid (left)	
Maximum length (along longitudinal axis)	40.5
Ectopterygoid (right)	
Maximum length of medial flange	35.2
Width (medial edge to lateral margin of lateral process)	31.3
Palatine (left)	
Maximum anteroposterior length	69.6
Height (dorsal border of anterio flange to distal tip of ventral peglike process)	43.4
Vomer (left)	
Maximum length	56.3

TABLE 3. Selected measurements (mm) of the braincase of AMNH FARB 6810.

Frontal	
Length (along interfrontal suture)	66.7
Mediolateral width (between distal ends of postorbital processes of both frontals)	101.3
Parietal	
Length (frontal-parietal suture to distal end of posterior left process)	75.5
Mediolateral width (between distal ends of posterior processes)	84.9
Braincase	
Length (distal end of parasphenoid to posteroventral margin of basioccipital)	128.8
Maximum length (distal end of parasphenoid to posterior end of left paroccipital process)	152.8
Mediolateral width (between distal end of paroccipital processes)	82.2
Mediolateral width of basisphenoid (between lateroventral ends of basipterygoid processes)	43.5
Mediolateral width (across sphenooccipital tubera)	35.2
Anteroposterior length of parasphenoid	69.6
Maximum height (dorsal apex of supraoccipital to ventral edge of left basipterygoid process)	92.1

2010). These new findings have led to new hypotheses on the evolutionary biology of early sauropodomorph dinosaurs (Yates, 2003a; Upchurch et al., 2007; Martínez and Alcober, 2009; Sertich and Loewen, 2010; Yates et al., 2010). The present study aims to complement Galton's treatment of AMNH FARB 6810 in particular, and the cranial anatomy of *Plateosaurus* in general. This is achieved by providing a more comparative approach in the context of the cur-

TABLE 4. Selected measurements (mm) of mandibular elements of AMNH FARB 6810.

Mandible (right, articulated)	
Total length (anterior end of dentary to posterior end of articular)	326.2
Height (dorsal margin of coronoid eminence to ventral border of angular)	53.4
Dentary (right)	
Length (anterior end to posteroventral tip)	176.8
Maximum depth of posterior region	39.7
Surangular (right)	
Maximum anteroposterior length	149.4
Maximum height (dorsal margin of coronoid eminence to ventral margin at articulation with angular)	45.2
Angular (right)	
Maximum anteroposterior length	97.6
Maximum height (of posterior half)	14.2
Splenial (right)	
Maximum length (along ventral margin border)	107.1
Height (between distal ends of posterodorsal and posteroventral processes)	43.3
Intercoronoid (right)	
Maximum anteroposterior length	95.8
Coronoid (right)	
Length (along longitudinal axis)	35.2
Prearticular (right)	
Maximum anteroposterior length	151.7
Maximum height (of anterior region)	31.0
Articular (right)	
Maximum anteroposterior length	45.9
Maximum mediolateral width	27.6

rent taxonomic diversity of basal sauropodomorphs, with an emphasis on the morphology of the individual skull elements (in contrast to Galton's focus on sutural relationships) and a more detailed photographic documentation of the available fossil material. Selected measurements of the cranial elements are given in tables 1–4.

Von Huene collected the specimen in July of 1925. According to AMNH catalog records he received $1500 to conduct an expedition in the Trossingen area. This field trip resulted in the collection of two skeletons; collection records indicate "we took the best one." On arrival in New York, H. Dehlin carefully prepared the specimen (fig. 1) and a cast (fig. 2) was made of the skull before Charles Lang mounted the entire specimen (except for the articulated skull, which is a

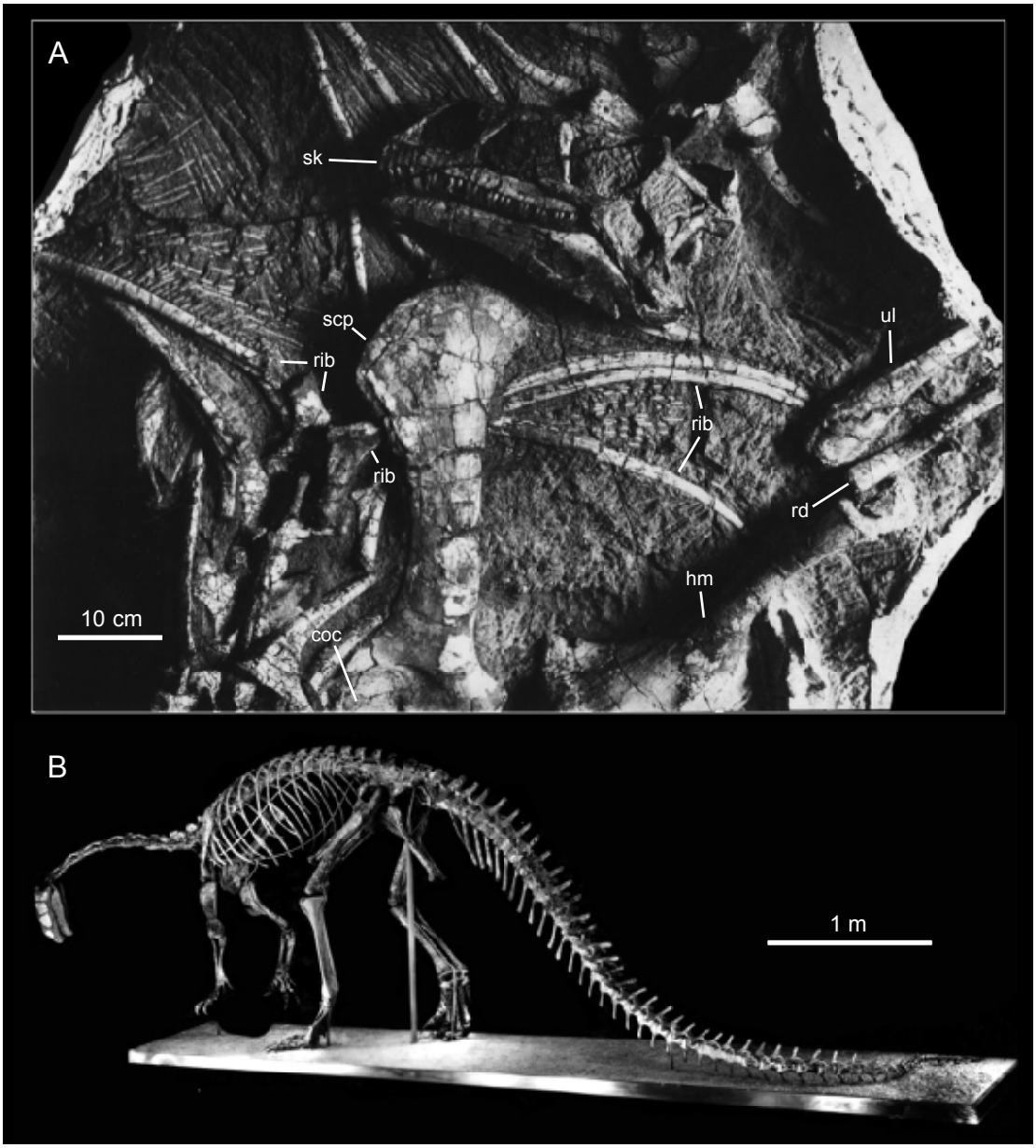

FIG. 1. Skull and partial postcranium of *Plateosaurus erlenbergiensis* (AMNH FARB 6810). **A,** field jacket containing the skull and postcranial elements still partially embedded in thr rock matrix; **B,** mounted skeleton in left lateral (and slightly posterior) view. Abbreviations in appendix 2.

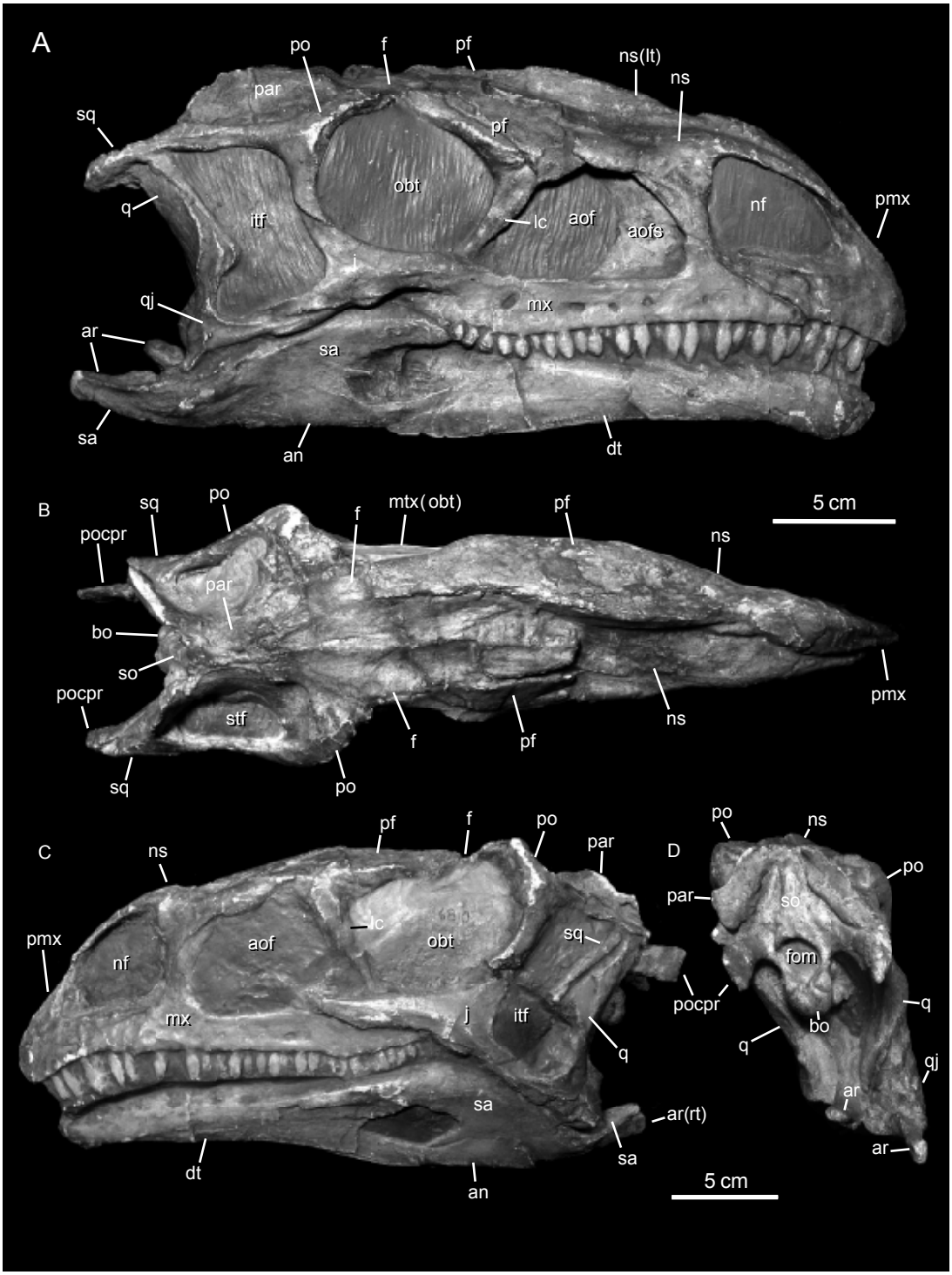

FIG. 2. Cast of the articulated skull of *Plateosaurus erlenbergiensis* (AMNH FARB 6810). **A,** right lateral; **B,** dorsal; **C,** left lateral; **D,** posterior. Abbreviations in appendix 2.

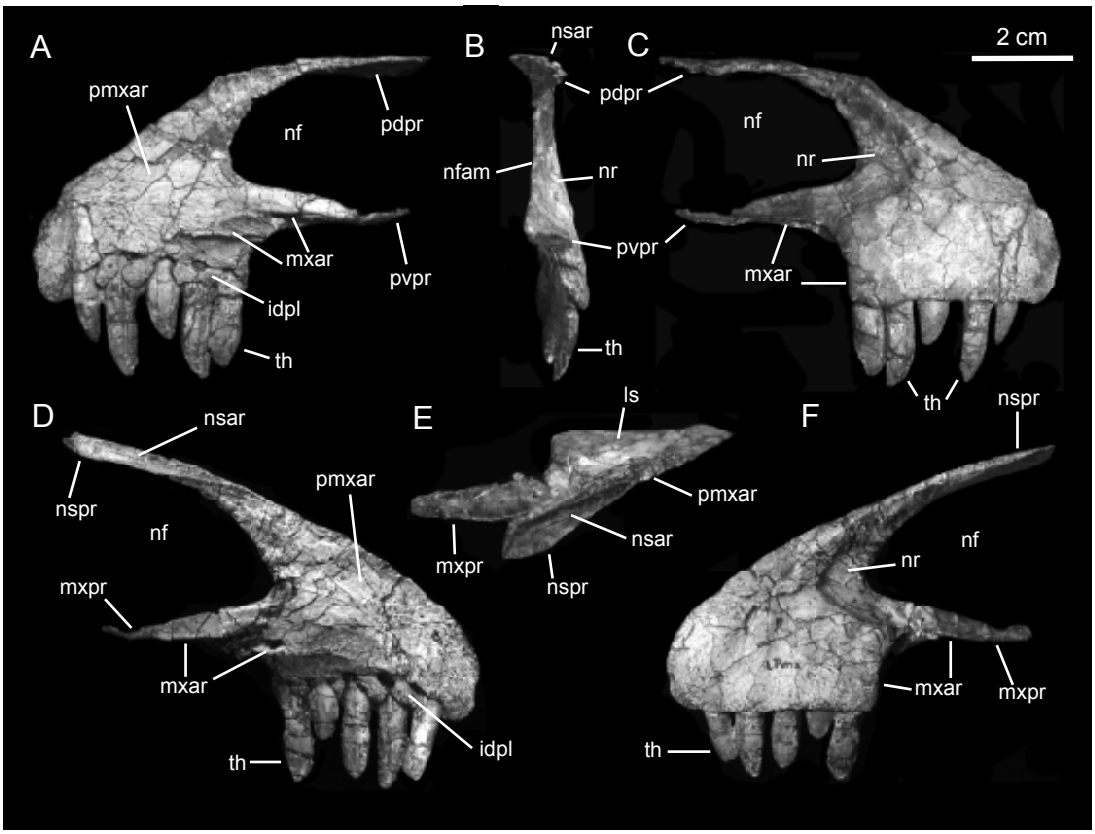

FIG. 3. Premaxillae of *Plateosaurus erlenbergiensis* (AMNH FARB 6810). **A,** medial; **B,** anterior; and **C,** lateral views of right premaxilla. **D,** medial; **E,** dorsal; and **F,** lateral views of left premaxilla. Abbreviations in appendix 2.

cast) in 1934. The specimen (fig. 1B) is still on display in the David H. Koch Hall of Saurischian Dinosaurs at the American Museum of Natural History, with a cast skull based on the now disarticulated remains. The other specimen collected by von Huene is one of two specimens on display at Institute for Geosciences of the Eberhard-Karls-University Tübingen, Germany.

REDESCRIPTION OF AMNH FARB 6810

Facial Skeleton

Premaxilla: The premaxilla forms the anterior end of the snout, partially encloses the narial fenestra and its ventral margin bears the premaxillary tooth row (fig. 2A). As in many other basal saurpodomorphs like *Unaysaurus tolentinoi* (Leal et al., 2004) and *Yunnanosaurus huangi* (Young, 1942), the premaxilla is triangular, mediolaterally compressed and has two posterior rodlike processes that enclose the anterior region of the narial fenestra (fig. 3). The main premaxillary body is slightly longer anteroposteriorly than dorsoventrally, as in *Anchis-*

aurus polyzelus (Galton, 1976; Yates, 2010), *Thecodontosaurus caducus* (Yates, 2003a) or *Yunnanosaurus huangi* (Barrett et al., 2007) but unlike *Mussaurus patagonicus* (Pol and Powell, 2007). The posterodorsal region of the lateral surface of the premaxilla contains a D-shaped recessed surface that borders anteriorly the narial opening and constitutes the narial fossa (fig. 3C, F). Anteriorly and adjacent to the low ridge that bounds the narial fossa there is a deep, oval foramen. There is also a minute neurovascular foramen on the anterior region of the lateral surface, just above the level of the posterior carina of the first premaxillary tooth, that is clearly visible in the right premaxilla and probably also present in the left one. The subnarial foramen lies on the posterior margin of the main body of the premaxilla, ventral to the narial fossa. The foramen is bounded by the nasal anteriorly and the articulating premaxilla posteriorly. The foramen is relatively small in size and slightly elongated dorsoventrally.

The medial surface of the main body of the premaxilla is flat where it articulates with its counterpart (fig. 3A, D). In ventral view, this medial surface forms a 20° angle to the tooth row, so that when both premaxillae are articulated they form V-shaped dorsal and ventral profiles. The region medial to the last three premaxillary teeth forms a recessed and flattened facet that faces medioventrally. This facet is separated dorsally from the flat medial premaxillary articulation surface by a sharp ridge (fig. 3A, D). This ridge is as long as the combined width of the last three teeth and provides a mediolaterally short shelf for supporting the anteromedial process of the maxilla.

The dorsal margin of the main body of the premaxilla forms a sharp edge that anteroventrally slopes to form an angle of 35° with the alveolar margin of the tooth row, an angle that is indicative of a relatively low snout as in *Yunnanosaurus huangi* (Barrett et al., 2007) but unlike forms such as *Unaysaurus tolentinoi* (Leal et al., 2004), *Mussaurus patagonicus* (Pol and Powell, 2007), and *Aardonyx celestae* (Yates et al., 2010). At the anterior end, this margin curves further ventrally to form a blunt lateral profile in the anterior end of the snout. Of the two processes that project posteriorly from the main body of the premaxilla, the ventral one extends horizontally to about middepth of the main body of the premaxilla underlying the narial fenestra. This posteroventral process is dorsoventrally compressed and gradually narrows posteriorly. Its dorsal (and slightly lateral) surface is concave longitudinally, as part of the recessed surface located anterior and adjacent to the narial opening. Two additional facets are present on this process, one ventral and a narrower one medially. The ventral surface has a longitudinal and sharp ridge, positioned near the lateral margin of the process. This ventral surface is rugose and rests over the anterodorsal shelf of the maxilla. Unlike in *Unaysaurus tolentinoi* (Leal et al., 2004) a foramen is not present on the ventral surface of the posteroventral process of the premaxilla.

The second process of the premaxilla extends posterodorsally from the dorsal edge of the main body of the element, bounding most of the anterior and anterodorsal region of the external naris. The medial surface of the proximal region of this process is flat and continuous with the medial side of the main body of the premaxilla. Posteriorly from its broad proximal base, the process becomes dorsoventrally compressed, extremely thin, and mediolaterally wide distally. A narrow and longitudinal recessed surface, located laterally on the dorsal surface of the distal segment of the posterodorsal process, constitutes the articular facet for the thin anteroventral process of the nasal (fig. 3D).

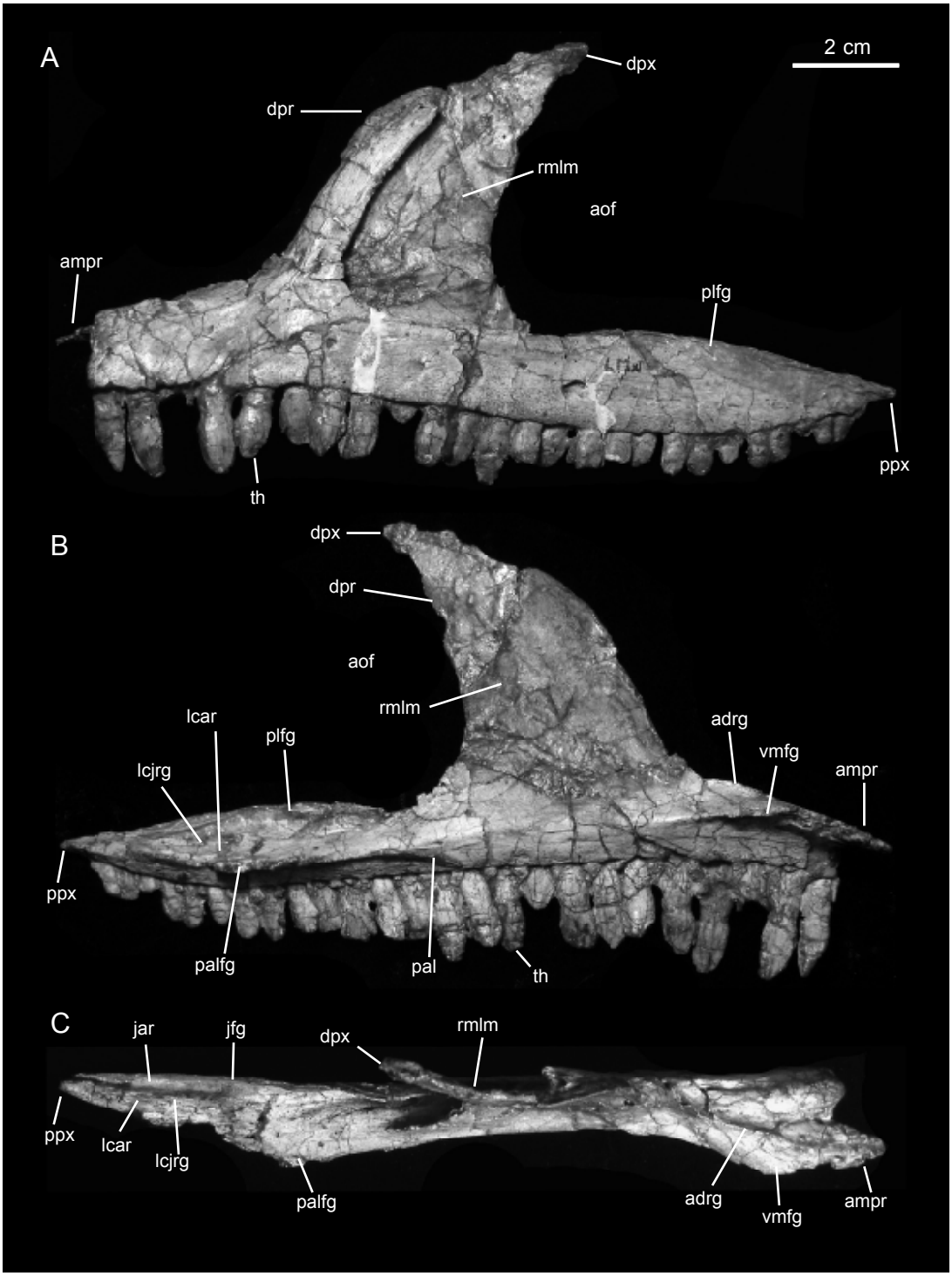

FIG. 4. Left maxilla of *Plateosaurus erlenbergiensis* (AMNH FARB 6810). **A,** lateral; **B,** medial; **C,** dorsal. Abbreviations in appendix 2.

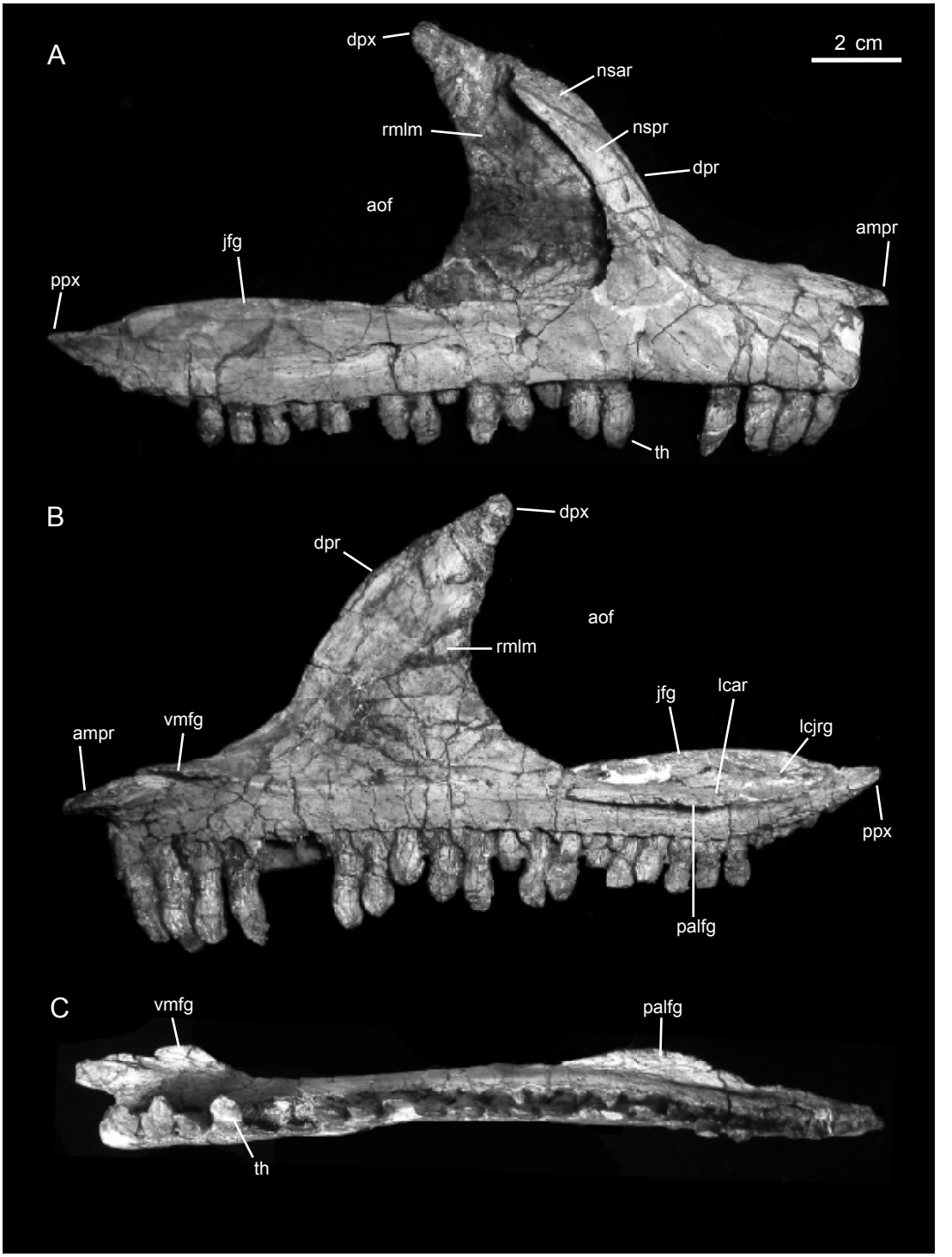

FIG. 5. Right maxilla of *Plateosaurus erlenbergiensis* (AMNH FARB 6810). **A,** lateral; **B,** medial; **C,** ventral. Abbreviations in appendix 2.

Each premaxilla has five teeth, a tooth count present also in *Aardonyx celestae* (Yates et al., 2010). According to Huene (1926) and Galton (1984), in rare occasions other specimens (e.g., SMNS 13200) and species of *Plateosaurus* may show up to six premaxillary teeth; this high tooth count may constitute an autapomorphy for the genus. Medially, large and triangular interdental plates are found in between each consecutive tooth (fig. 3A, D). Above these plates, the alveolar margin is more dorsally located relative to that of the lateral side of the premaxilla. While the lateral alveolar margin of the tooth row is horizontally oriented, that of the medial side arches dorsally above the second tooth. The tips of replacement teeth can be seen still embedded inside the alveoli, dorsal and slightly medial to the erupted teeth.

Maxilla: The maxilla is mediolaterally compressed and as in other basal sauropodomorphs (Galton and Upchurch, 2004), it has a triradiate lateral profile consisting of two major parts: a horizontal main ramus bearing the tooth row and a dorsal process (figs. 4, 5). The main ramus is dorsoventrally shallow and is divided into three segments: the segment anterior to, that immediately below, and that posterior to the dorsal process. The lateral surface of the ventral ramus is flat and oriented vertically, lying nearly in the same plane as the lateral surface of the tooth crowns. In contrast, the medial side of the main ramus is dorsoventrally convex due to the presence of a longitudinal median ridge (figs. 4B, 5B). Although it is much less prominent ventral to the base of the dorsal process, this ridge is continuous along the entire length of the maxilla. Such a ridge has also been observed in other basal sauropodomorphs, like *Massospondylus carinatus* (Gow et al., 1990) and *Aardonyx celestae* (Yates et al., 2010).

Along the anterior segment of the main ramus, the median ridge becomes more prominent and forms a dorsomedial process (fig. 4B, C). This process projects anteriorly a short distance beyond the anterior end of the maxillary ramus. It also extends mediodorsally forming a narrow platform. The ventralmost posterior process of the premaxilla overlaps the lateral half of this platform; the medial half of the platform contacts the vomer. The anterior end of the maxilla is subquadrangular in lateral view, as in other basal sauropodomorphs like *Riojasaurus incertus* (Bonaparte and Pumares, 1995), *Mussaurus patagonicus* (Pol and Powell, 2007), and *Aardonyx celestae* (Yates et al., 2010). It consists of a vertical mediolaterally compressed surface. This surface is slightly concave medially and contacts the posterior side of the main body of the premaxilla, below the posterior process of the latter.

The dorsal process of the maxilla rises from the dorsal surface of the ventral ramus as a triangular, finlike lamina (fig. 4A, B). The base of the dorsal process comprises about 35% of the length of the maxilla and its midlength is found anterior to the midlength of the maxilla. Most of the surface of the dorsal process forms the lateral wall of the antorbital fossa. This antorbital region is medially recessed relative to the lateral surface of the anterior margin of the dorsal process and the lateral wall of the maxilla. The anterolateral region of the dorsal process forms an anteroposteriorly thick border that is continuous ventrally with the lateral surface and the anterodorsal shelf of the maxilla. This anterior border gradually thins dorsally, wedging and curving posterodorsally to form a sharp apex. This apex, however, does not reach the summit of the lamina of the dorsal process. The anteriormost edge of the dorsal process shows a narrow facet that is overlapped by the medioventral region of the nasal (fig. 5A). This

facet faces more anteriorly than laterally and can be followed along the entire anterior edge of the dorsal process. The entire medial surface of the dorsal process is slightly concave ventrally, and continuous with the medial wall of the maxilla.

Slightly anterior to the midlength of the maxillary main ramus, the dorsal margin of the lateral surface is sharply defined (figs. 4A, 5A) and separated from the base of the dorsal process of the maxilla by a deep groove. This groove, which lies at the floor of the antorbital fossa, has been identified in other basal saurpodomorphs like *Pantydraco caducus* (Yates, 2003a; Galton et al., 2007; Galton and Kermack, 2010), *Massospondylus carinatus* (Gow et al., 1990), and *Mussaurus patagonicus* (Pol and Powell, 2007). According to Witmer (1997) this groove transmitted the maxillary nerve.

The lateral surface of the posterior third of the ventral ramus of the maxilla is dorsoventrally deeper than that of the middle third (figs. 4A, 5A). At the posterior end of the maxilla, the dorsal and ventral margins of the lateral surface converge to form a sharp apex. The dorsal margin of the lateral surface of the posterior segment of the maxilla is sharp as a continuation of the dorsal margin of the central segment, to form a narrow and elongated flange (fig. 4A, B). Medial to this flange, the ventral ramus expands medially and the median longitudinal ridge becomes very prominent (figs. 4B, 5B), contacting the palatine. Posteriorly, the median ridge becomes gradually less expanded to merge with the posterior apex of the maxilla. Ventral to the median flange and adjacent to the alveolar margin the medial side of the maxilla faces medioventrally. The dorsal surface of the posteriormost portion of the maxilla, between the posterolateral flange and the median ridge, is bisected by a long, sharp, and shallow "lacrimojugal" ridge (fig. 4B, C). The surfaces lateral and medial to this ridge are strongly concave. The surface lateral to the ridge receives the anterior segment of the anterior ramus of the jugal; the medial surface receives the ventral process of the lacrimal.

The left maxilla has 25 tooth positions and the right 24. The medial margin of the alveoli are dorsally offset relative to the lateral margin. Arrow-shaped interdental plates lie between consecutive teeth. These plates are one-fifth to one-fourth of the length of tooth crowns. The lateral surface of the ventral ramus of each maxilla is pitted with eight neurovascular foramina (figs. 4, 5). Similar foramina are also present in basal sauropodomorphs, but their number differs: for example, there are five foramina in *Pantydraco caducus* (Yates, 2003a) and six in *Lufengosaurus huenei* (Barret et al., 2005) and *Mussaurus patagonicus* (Pol and Powell, 2007).

Nasal: The paired nasals are thin laminae of bone roofing the laterodorsal surface of the snout and the anterodorsal region of the skull (fig. 2). In contrast to other basal sauropodomorphs, each nasal of AMNH FARB 6810 is longer than half the length of the skull roof (Galton and Upchurch, 2004). In *Efraasia minor*, each nasal is very elongate, but only about half as long as the length of the skull roof (Yates, 2003b: text-fig. 9). The nasal of *Plateosaurus* is curved laterodorsally. Both nasals in AMNH FARB 6810 lack parts of the posteromedial regions that articulate with the frontal and prefrontal bones. Overall, this bone consists of a subrectangular dorsal lamina and two anteroventrally projecting processes (figs. 6, 7). These processes form the dorsal, posterior, and posterodorsal margins of the narial fenestra. The ventral margin of the nasal slightly arches and overlaps the anterior border of the dorsal process of the maxilla (fig.

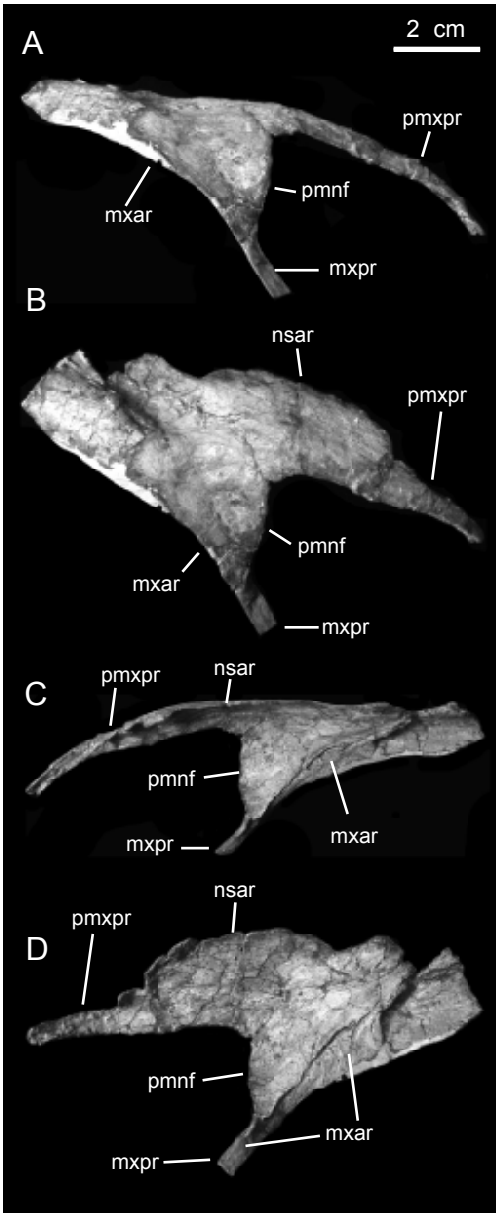

FIG. 6. Right nasal of *Plateosaurus erlenbergiensis* (AMNH FARB 6810). **A,** lateral; **B,** dorsal; **C,** medial; **D,** ventral. Abbreviations in appendix 2.

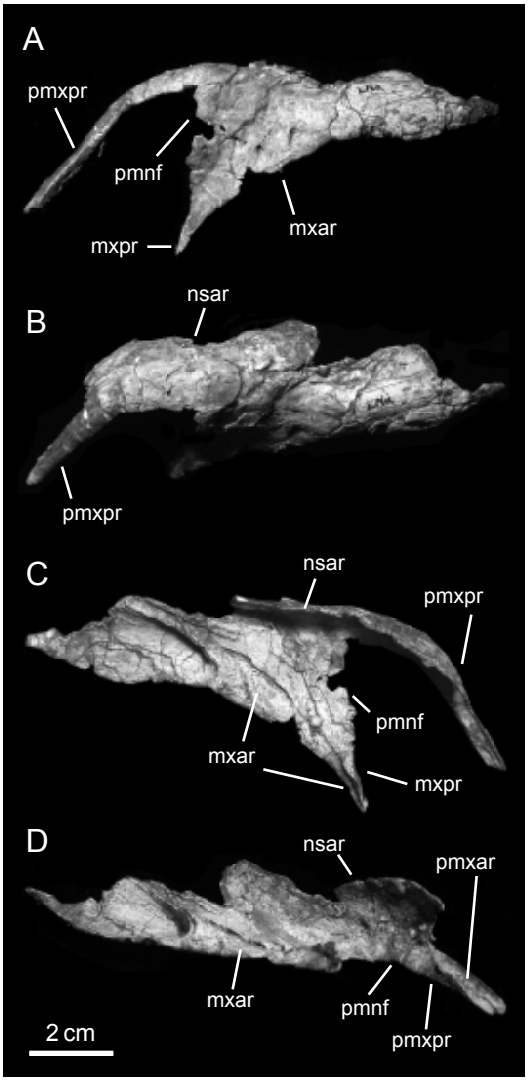

FIG. 7. Left nasal of *Plateosaurus erlenbergiensis* (AMNH FARB 6810). **A,** lateral; **B,** dorsolateral; **C,** medial; **D,** ventromedial. Abbreviations in appendix 2.

2). In doing so, the ventral margin of the nasal contributes to the anterodorsal border of the antorbital fossa and its concave medial surface encloses a narrow cavity formed in conjunction with the dorsal region of the dorsal process of the maxilla. Notably, the nasal contribution to the dorsal margin of the antorbital fossa is relatively extensive (fig. 2), as in *Riojasaurus incertus* (Bonaparte and Pumares, 1995). This contrasts with the condition in other basal sauropodo-

morphs like *Lufengosaurus huenei* (Barrett et al., 2005), *Mussaurus patagonicus* (Pol and Powell, 2007), and *Anchisaurus polyzelus* (Yates, 2004) where the dorsal margin of the antorbital fossa is reduced and forms an apex.

The dorsal lamina of the nasal projects laterodorsally. Anteriorly, this lamina is continuous with the proximal region of the anterodorsal process. Anteroventrally, the lamina merges with the proximal region of the anteroventral process. The posterior half of the lateral surface of the dorsal lamina of the nasal contains two distinct subrectangular regions, the long axes of which are obliquely (anteroventrally) oriented (fig. 6B). The most anterior of these is recessed relative to the surrounding bone, whereas the adjacent, posteriormost region is slightly convex laterally. Its medial surface is very concave and laterally recessed relative to the surrounding areas (fig. 6C, D), containing sharp and well-developed ridges bounding its anterodorsal and anteroventral margins. The medial surface of the anteroventral margin of the nasal is flat and slightly arched anteroposteriorly. A long and sharp ridge separates this medial surface from the remaining area of the nasal above. Both the latter medial surface, and the posterodorsal medial recessed region overlap the anterodorsal margin of the dorsal process of the maxilla (figs. 6C, 7C).

The proximal half of the anterodorsal process of the nasal is very broad. Distally, the process becomes abruptly narrow and finger-like (fig. 6B). The medial surface of the broad proximal region of the anterodorsal process is concave. The medial side of the distal segment contains an oblique and recessed facet widen-

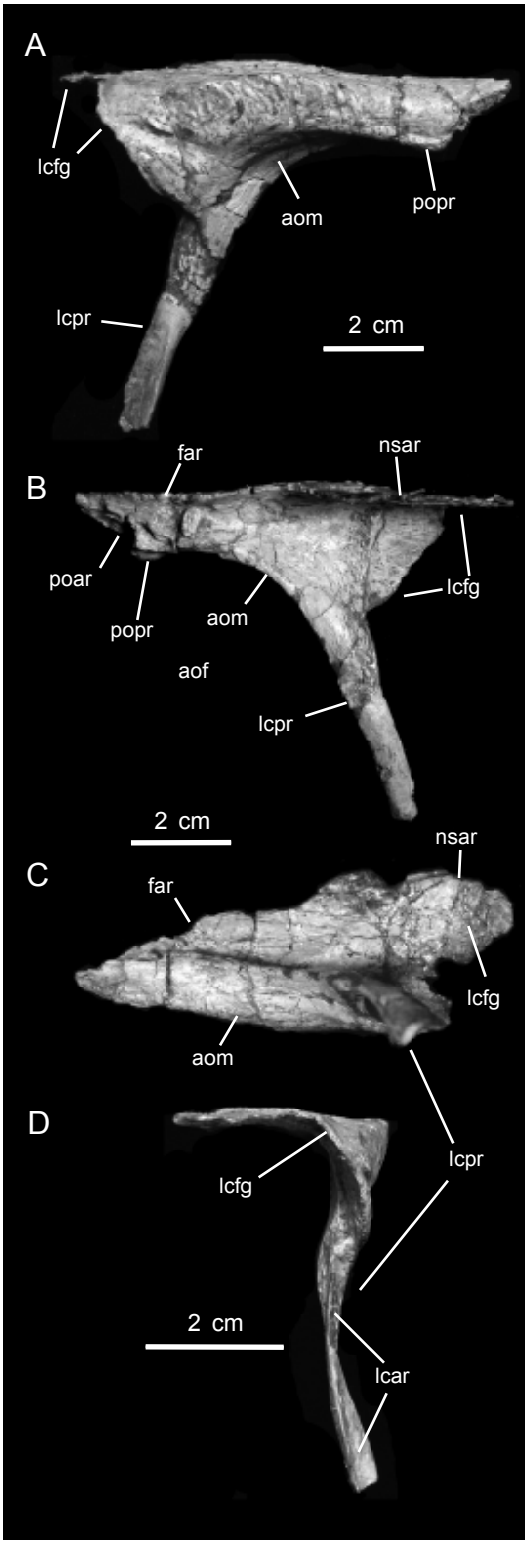

FIG. 8. Left prefrontal of *Plateosaurus erlenbergiensis* (AMNH FARB 6810). **A,** lateral; **B,** medial; **C,** medial; **D,** posterior. Abbreviations in appendix 2.

ing anteriorly (fig. 6C, D). This facet overlaps the posterodorsal process of the premaxilla.

The anteroventral process of the nasal has a triangular proximal region and its lateral surface is slightly depressed. The anterior and posteroventral margins of the proximal region of this process converge ventrally to form a narrow distal segment (fig. 6A). The distalmost termini of this segment are missing in both nasals of AMNH FARB 6810. The ventral border of the anteroventral process overlaps a narrow recessed margin of the dorsal process of the maxilla, as well as part of the lateral margin of the anterodorsal maxillary shelf further distally. The distal segment of the anteroventral process of the nasal slightly twists distally, so that its lateral surface faces more anteriorly near its distal end. There, the process is overlapped by the equally thin posterior process of the premaxilla.

Prefrontal: The prefrontal is a T-shaped element forming the anterodorsal margin of the orbit (fig. 2). It is composed of a horizontal dorsomedial flange, the surface of the lateral orbital rim, and a ventral, rod-shaped ramus (figs. 8, 9). The mediodorsal flange consists of a thin lamina of bone extending medially from the orbital rim. The width of this lamina is variable among basal sauropodomorphs; it is less extensive in *Mussaurus patagonicus* (Pol and Powell, 2007). The dorsal surface of this lamina is nearly flat forming a 90° angle to the thick lateral surface of the dorsal orbital margin. The anterior region of the dorsomedial lamina of the prefrontal is very thin (fig. 8B) overlapping the convex posterodorsal surface of the lacrimal extensively (fig. 2). In addition, the lamina would contact the nasal anterome-

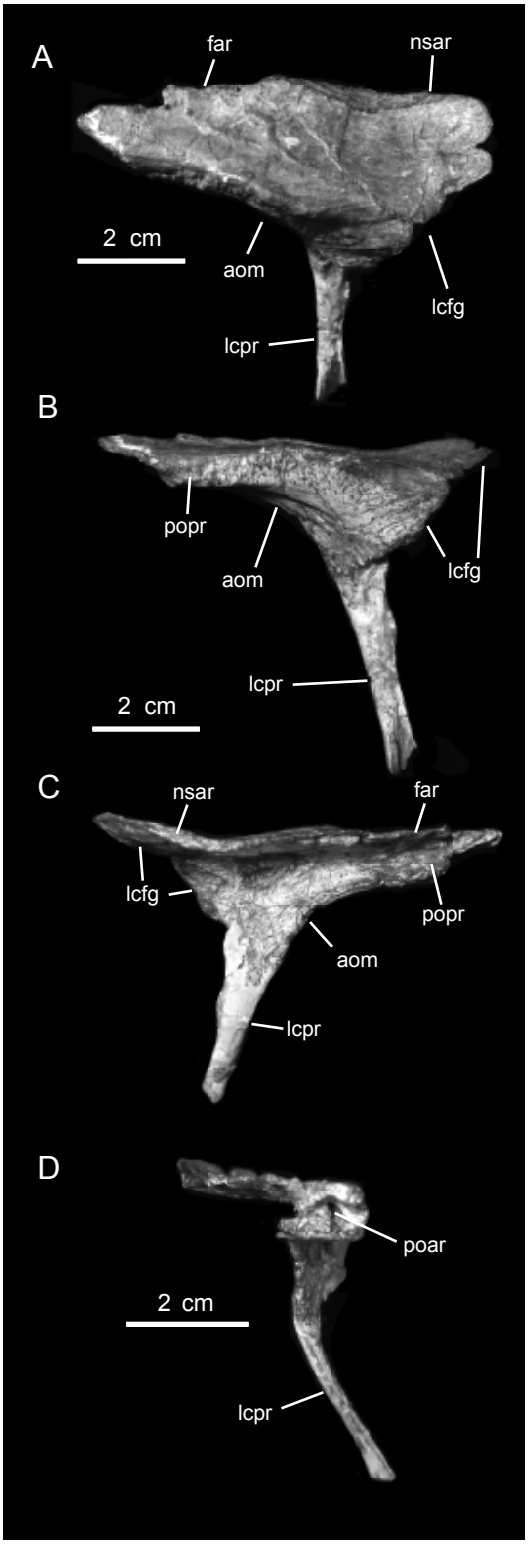

FIG. 9. Right prefrontal of *Plateosaurus erlenbergiensis* (AMNH FARB 6810). **A,** dorsal (and slightly lateral); **B,** lateral; **C,** medial; **D,** anterior. Abbreviations in appendix 2.

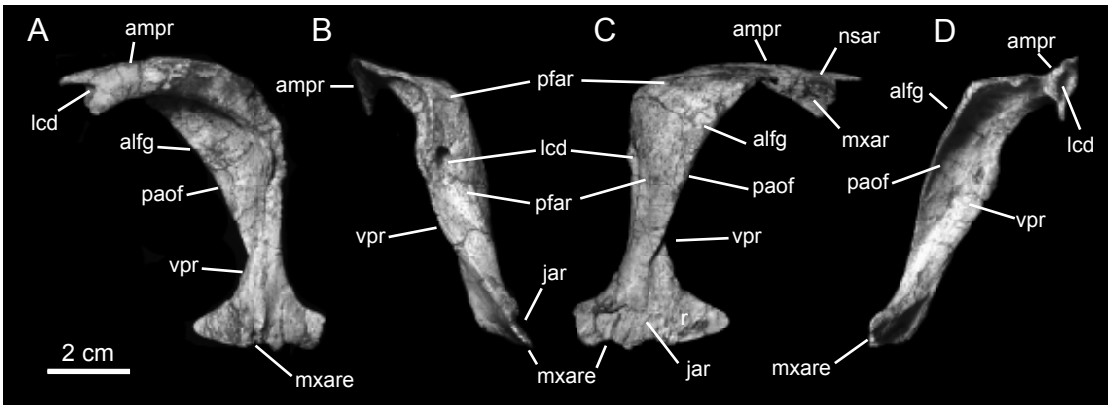

FIG. 10. Right lacrimal of *Plateosaurus erlenbergiensis* (AMNH FARB 6810). **A,** medial; **B,** posterior; **C,** lateral; **D,** anterior. Abbreviations in appendix 2

dially; however, the anatomical details of the prefrontal-nasal joint are uncertain because the anterior region of the prefrontal incompletely preserved in AMNH FARB 6810. In dorsal view, the medial lamina constricts posteriorly at the contact with the frontal (figs. 8C and 9A). The medial edge of the posterior region of the dorsomedial lamina interdigitates with the frontal. Posteriorly, the dorsal region of the prefrontal thickens dorsoventrally and contains a narrow socket for reception of the anterior ramus of the postorbital (fig. 9D). The dorsal region of the prefrontal does not extend posteriorly as much as in *Anchisaurus polyzelus* (Yates, 2010) but more so than in forms like *Coloradisaurus brevis* (Bonaparte, 1978). The laterodorsal surface of the prefrontal contributing to the orbital margin is gently curved and shows fine vertical striations. Anteriorly, the orbital margin greatly expands ventrally and is triangular in lateral view, bounding the anterodorsal corner of the orbit (figs. 8A, 9B). This region shows obliquely oriented striations.

The ventral ramus of the prefrontal forms is angled ~110° relative to the orbital margin. The ramus slightly tilts laterally from the parasagittal plane of the skull (fig. 9A, D). The anterior margin of the ramus articulates into a long groove on the medial side of the lacrimal shaft. Distally, the ventral ramus of the prefrontal slightly twists anteromedially and contains a shallow groove receiving a ridge of the medial surface of the distal region of the shaft and ventral process of the lacrimal (fig. 8D).

Lacrimal: The lacrimal bounds the posterodorsal region of the antorbital fenestra (fig. 2). In lateral and medial views, the lacrimal has the outline of an inverted "J" (figs. 10, 11). The main shaft of the lacrimal is compressed anteroposteriorly and separates the orbit posteriorly from the antorbital fenestra (fig. 2A). Its medial side has a large and long groove for reception of the ventral ramus of the prefrontal. Adjacent to this groove on the posterior surface of the shaft lies the large opening for the lacrimal duct (figs. 10B, 11B), which is located at midway down the shaft and gradually deepens dorsally.

The dorsal region of the lacrimal anteroventrally projects forming a 90° angle to the shaft along its antorbital margin (fig. 11A, C). The medial surface of the anteroventral region of the

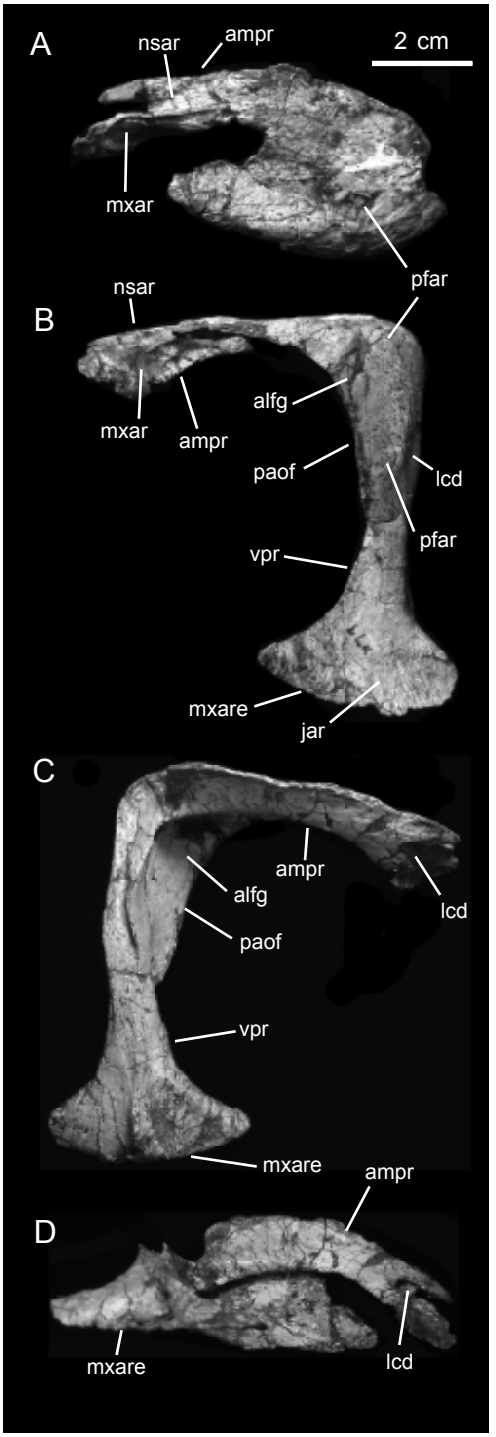

FIG. 11. Left lacrimal of *Plateosaurus erlenbergiensis* (AMNH FARB 6810). **A,** dorsal; **B,** lateral; **C,** medial; **D,** ventral. Abbreviations in appendix 2.

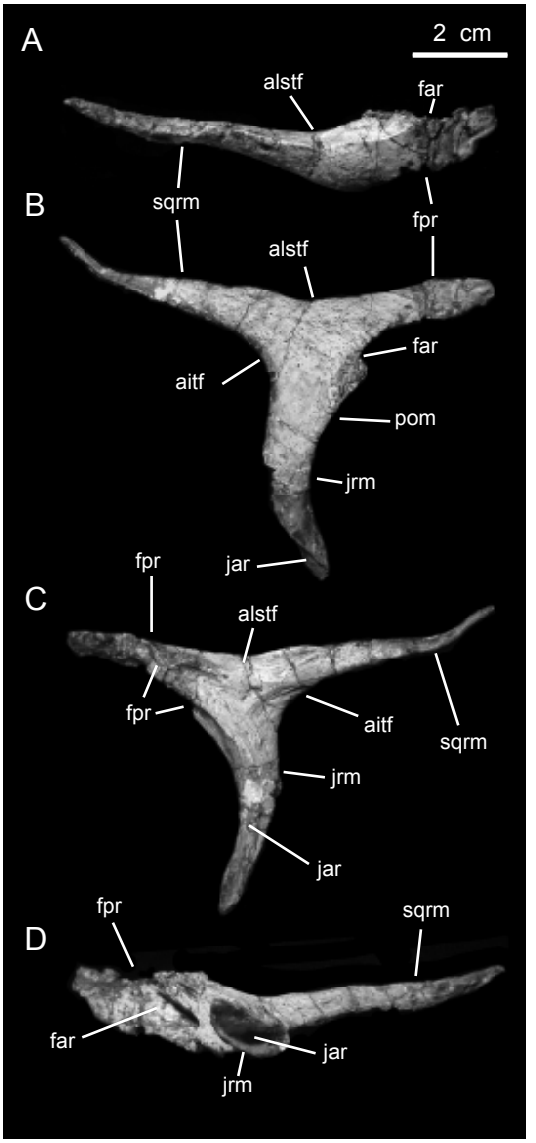

FIG. 12. Right postorbital of *Plateosaurus erlenbergiensis* (AMNH FARB 6810). **A,** dorsal; **B,** lateral; **C,** medial; **D,** ventral. Abbreviations in appendix 2.

lacrimal is a concave and narrow facet that is proximally continuous with the articular groove for the prefrontal. More anteriorly, the medial facet is flat and medioventrally oriented (fig. 11C). This surface probably articulated with the lateral region of the nasal (an area of this bone not preserved in AMNH FARB 6810). The anterodorsal end of the lacrimal is a bifid process (fig. 11A). This process is dorsoventrally expanded and contains a small circular depression opening anteriorly (fig. 11D). This depression probably accommodated the posterodorsal tip of the dorsal process of the maxilla. The bifid process is triangular in cross section, with flat dorsal, medioventral, and lateral surfaces. The dorsal projection of the process is longer than the ventral one.

An important feature of the lacrimal is the large lateral flange that forms most of the posterodorsal margin of the antorbital fenestra (figs. 2, 11C). This flange is present in other basal sauropodomorphs, varying in degree of development (Barrett et al., 2005) but is absent in *Mussaurus patagonicus* (Pol and Powell, 2007). However, the great development that this flange achieves in *Plateosaurus erlenbergiensis* is autapomorphic for this taxon (Yates, 2003b). The lateral flange consists of a lamina that originates on the lateral side of the ventral region of the lacrimal shaft, just dorsal to the ventral process. From there, the flange anterolaterally expands and ascends obliquely (anterodorsally), forming an extensive convex laterodorsal surface and a corresponding deep depression on its medioventral surface (fig. 11A). Dorsomedially, the flange anteriorly curves to form a flat platform that roofs the antorbital fenestra. The posterodorsal region of the platform overlapped the anterodorsal flange of the prefrontal (fig. 2). Additionally, the anterior region of the platform was overlapped by the posterodorsal region of the nasal.

At the base of the lacrimal shaft there is a finlike, anteroposteriorly expanded process that slightly thickens posteriorly. The lateral surface of the ventral process of the lacrimal is vertically striated, suggesting that this area was overlapped by the distal segment of the anterior ramus of the jugal. The medial side of the ventral process is bisected by a short, thick, and vertical ridge. This ridge would nestle into a groove on the distal end of the ventral ramus of the prefrontal.

Postorbital: The postorbital is triradiate and forms the posterodorsal margin of the orbit and the anterodorsal corner of the infratemporal fenestra (figs. 2, 12, 13). The distal ends of the anterior rami are missing in both postorbitals, so that they would have been longer than preserved. A relatively long anterior ramus, with concomitant elevation of its distal region rela-

FIG. 13. Left postorbital of *Plateosaurus erlenbergiensis* (AMNH FARB 6810). **A,** lateral; **B,** posterior; **C,** medial; **D,** anterior. Abbreviations in appendix 2.

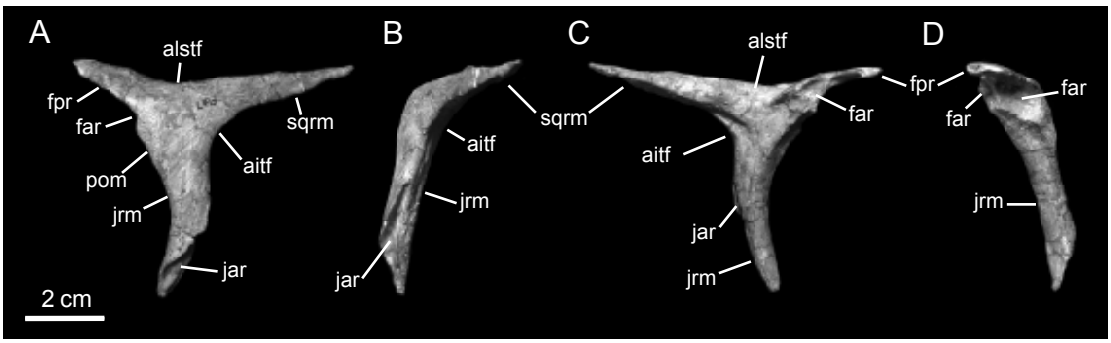

tive to the caudal ramus and lateral exposure of the supratemporal fenestra has also been reported in *Massospondylus* and *Yunnanosaurus* (Barrett et al., 2007). The anterior ramus of AMNH FARB 6810 is dorsoventrally compressed, projects anteriorly and slightly dorsally, and its dorsal margin forms an angle of 160° relative to the posterior ramus. In the proximal region of the ramus there is a flange extending medially from the mediodorsal border (fig. 12A, D). Anterolaterally from this flange, there is a deep excavation receiving a fingerlike posterolateral process of the frontal (figs. 12D, 13D). This articulation is laterally exposed and is accompanied by the insertion of the anterior postorbital ramus on the recessed dorsal surface of the posterolateral process of the frontal. In this way the postorbital and frontal form an interlocking joint. The lateral margin of the postorbital forms the posterolateral corner of the orbit displays various short and transverse striations giving the bone texture a rugose appearance (fig. 12).

Immediately below these striations, the ventral ramus of the postorbital articulates with the dorsal ramus of the jugal (fig. 12B, C). Proximally, the ventral ramus of the postorbital is mediolaterally expanded and triangular in cross section. It shows three facets proximally that are laterally, medially, and posteriorly oriented, respectively. The anterior and medial surfaces are separated by a ridge that is oriented obliquely. The distal half of the posterior surface of the ventral ramus contains a deep and narrow groove to receive the dorsal ramus of the jugal (fig. 13A, B). Distally, this groove opens onto the lateral surface of the distal third of the ramus (fig. 12D).

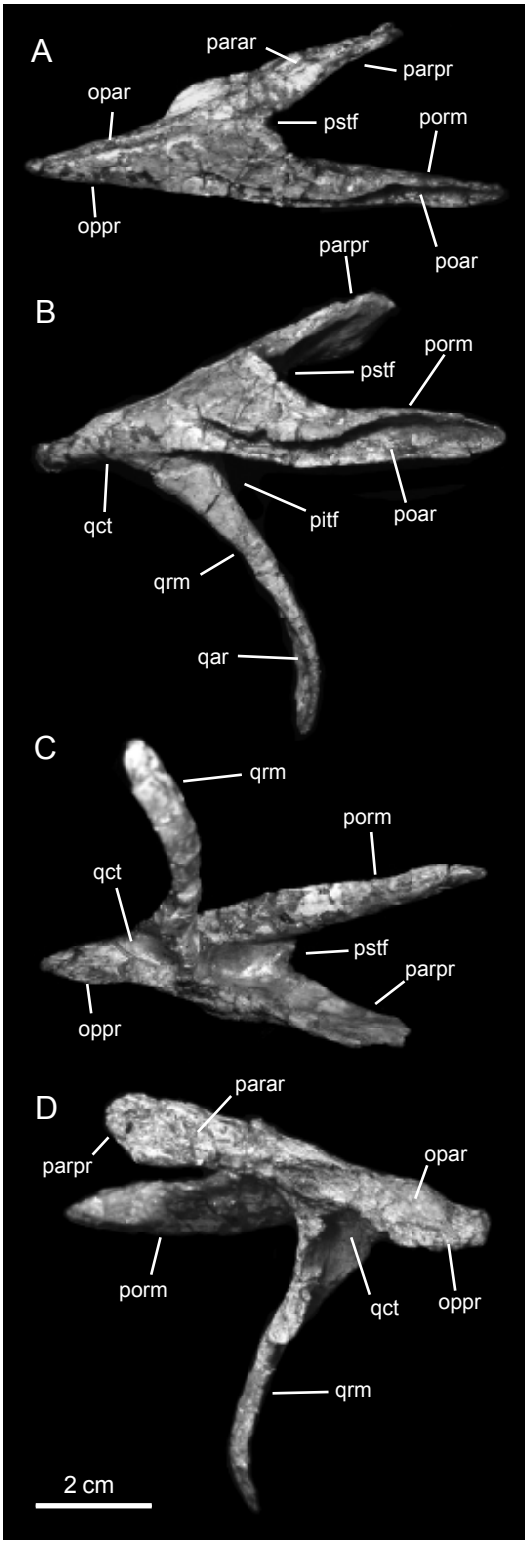

FIG. 14. Right squamosal of *Plateosaurus erlenbergiensis* (AMNH FARB 6810). **A,** dorsal; **B,** lateral; **C,** ventral; **D,** medial. Abbreviations in appendix 2.

The posterior ramus is mediolaterally compressed with a sharply defined dorsal edge (fig. 12A, B). Triangular in cross section, its ventral side is flat and narrow (fig. 12D). In the complete right postorbital the ventral ramus is long. Distally, the posterior ramus gradually tapers into sharp tip. Nearly the entire length of the ramus fits into a deep and long groove on the lateral side of the anterior ramus of the squamosal (fig. 2). The posterior ramus of the postorbital is relatively gracile in comparison with the stout and short ramus present in other basal sauropodomorphs like *Riojasaurus incertus* (Bonaparte and Pumares, 1995), *Lufengosaurus huenei* (Barrett et al., 2005), and *Yunnanosaurus huangi* (Barrett et al., 2007).

Squamosal: The squamosal is tetraradiate and contributes to the posterodorsal corner of the skull forming the posterodorsal region of the infratemporal fenestra (figs. 2, 14, 15). Three of the four rami lie anterior to the quadrate cotyle and extend ventrally, anteriorly, and anteromedially, respectively (fig. 14B). The fourth ramus is much shorter than the others and extends posteriorly from the quadrate cotyle. In dorsal and ventral views the anterolateral ramus forms an angle of 30° to the anteromedial ramus (fig. 14A).

The anterolateral ramus projects anteriorly and slightly ventrally from the laterodorsal border of the squamosal. It is mediolaterally compressed and substantially wider proximally. Its lateral surface contains a long and deep groove that receives the posterior ramus of the postorbital. This groove is distally wide, where it occupies the entire lateral surface of the ramus (fig. 14B). The medial side of the anterolateral ramus is dorsoventrally convex.

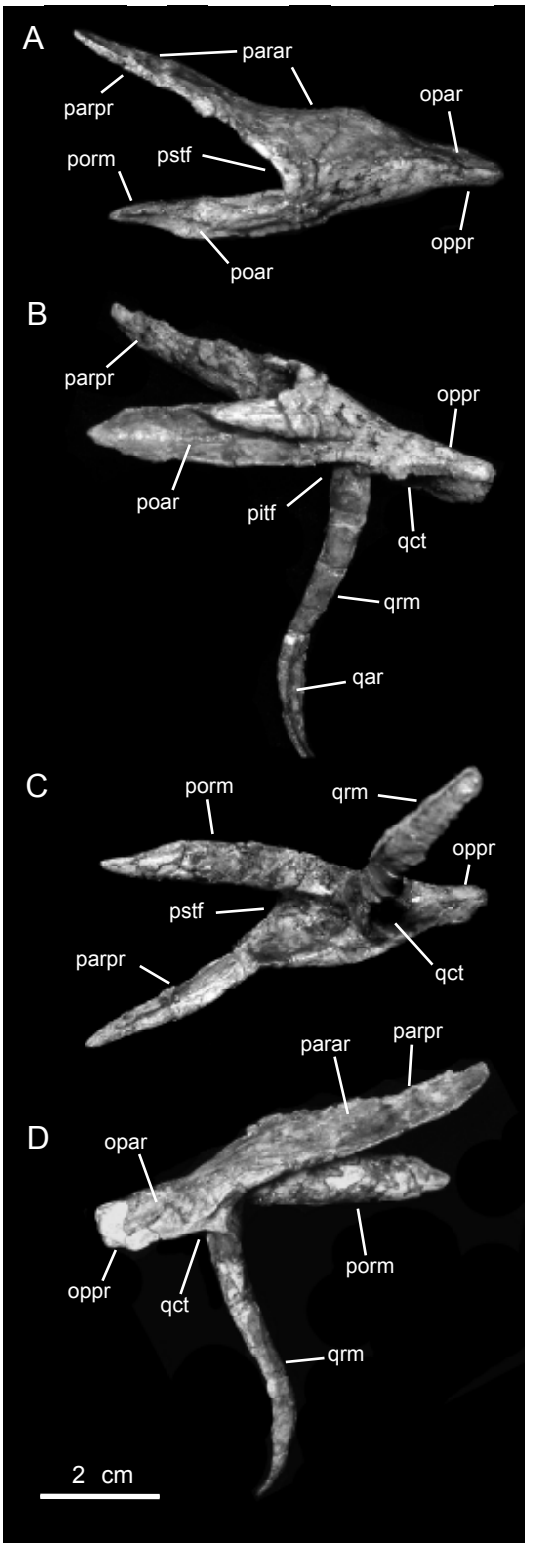

FIG. 15. Left squamosal of *Plateosaurus erlenbergiensis* (AMNH FARB 6810). **A,** dorsal; **B,** lateral; **C,** ventral; **D,** medial. Abbreviations in appendix 2.

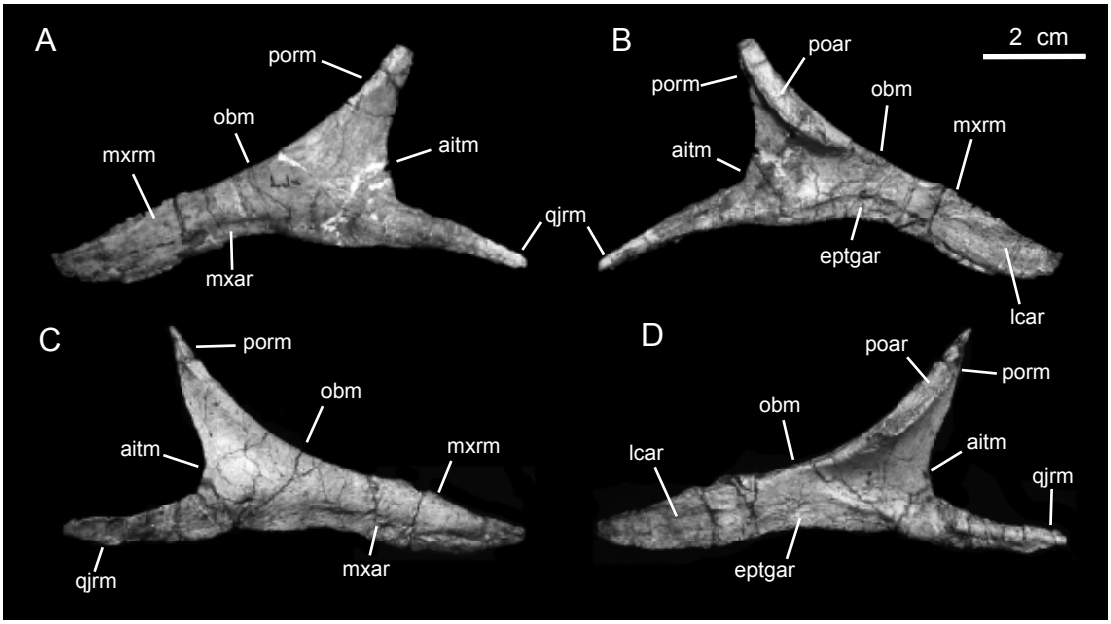

FIG. 16. Jugals of *Plateosaurus erlenbergiensis* (AMNH FARB 6810). **A,** lateral and **B,** medial views of left jugal. **C,** lateral and **D,** medial views of right jugal. Abbreviations in appendix 2.

The mediolaterally compressed anteromedial ramus is slightly expanded dorsoventrally at its anterior end. The medial surface of its posterior region contains an oblique ridge that extends into the dorsal margin of the posterior ramus of the squamosal (fig. 14D). This ridge constitutes the dorsal boundary of the articulation surface for the posterolateral process of the parietal. This articular surface is slightly concave and most of it is located on the medial side of the posterior ramus of the squamosal. This ramus is half as long as and as deep as the anteromedial ramus. The posterior ramus is mediolaterally compressed and forms the anterior, dorsal, medial, and posterior surfaces of the quadrate cotyle (fig. 14B, C). The ventral margin of this ramus forms a sharp edge posterior and medial to the quadrate cotyle.

The ventral ramus of the quadrate is the longest of all. It is longer than the total anteroposterior length of the element (i.e., the combined length of the posterior and anteromedial rami) (figs. 14B, 15B). It lies 90° to the dorsal margin of the squamosal. The proximal region of the ventral ramus is anteroposteriorly expanded and its posteromedial surface bounds the quadrate cotyle (fig. 14D). Distally, the posteromedial surface is longitudinally excavated by a long groove articulating with the lateral wing of the quadrate proximally and the quadratojugal distally (figs. 14B, 15B). The distalmost segment of the ventral ramus of the squamosal twists anterolaterally, exposing the segment of the groove laterally where it accommodates the anterodorsal ramus of the quadratojugal.

Jugal: The jugal is a Y-shaped bony lamina (fig. 16). The element is gently convex laterally. The anterior ramus is the longest, being twice as long as each of the other rami. The orbital margin delimited by the dorsal edges of the anterior and dorsal rami is smooth and gently concave (fig. 16A). These rami form a 145° angle with both jugals. In contrast, the infratem-

poral margin of the jugal, defined by the posterior border of the dorsal ramus and the dorsal border of the posterior ramus, has a V-shaped lateral profile. These rami meet at an 80° angle in the right jugal and 95° in the left one; obviously a preservational difference.

The lateral margin of the anterior ramus is gently convex dorsoventrally. The ventral surface of its distal half is rugose where it is overlapped by the medial surface of the posterior end of the maxilla (figs. 2, 16A, C). In contrast, the medial surface is slightly concave longitudinally and shows an elongate, D-shaped more concave and rugose facet for reception of the ectopterygoid (fig. 16B). Further anteriorly, the distal end of the medial surface of the anterior ramus overlaps the base of the lacrimal. Thus, the distal half of the anterior ramus of the jugal is sandwiched between the ventral process of the lacrimal and the posterior end of the maxilla (fig. 2) when in articulation.

The central area of the jugal, at the junction of the proximal region of the three rami, bulges laterally due to the presence of a corresponding medial oval depression (fig. 16D). Ventrally, this depression is separated by a longitudinal ridge from a recessed surface, which lies adjacent to the ventral margin of the jugal. This recessed surface contacts the ectopterygoid (fig. 16D).

The dorsal (postorbital) ramus is triangular and projects posterodorsally caudal to the midlength of the jugal (fig. 16). It is less inclined ventrally than in *Lufengosaurus huenei* (Barrett et al., 2005), *Mussaurus patagonicus* (Pol and Powell, 2007), *Massospondylus kaalae* (Barrett, 2009), and *Adeopapposaurus mognai* (Martínez, 2009), and comparable in

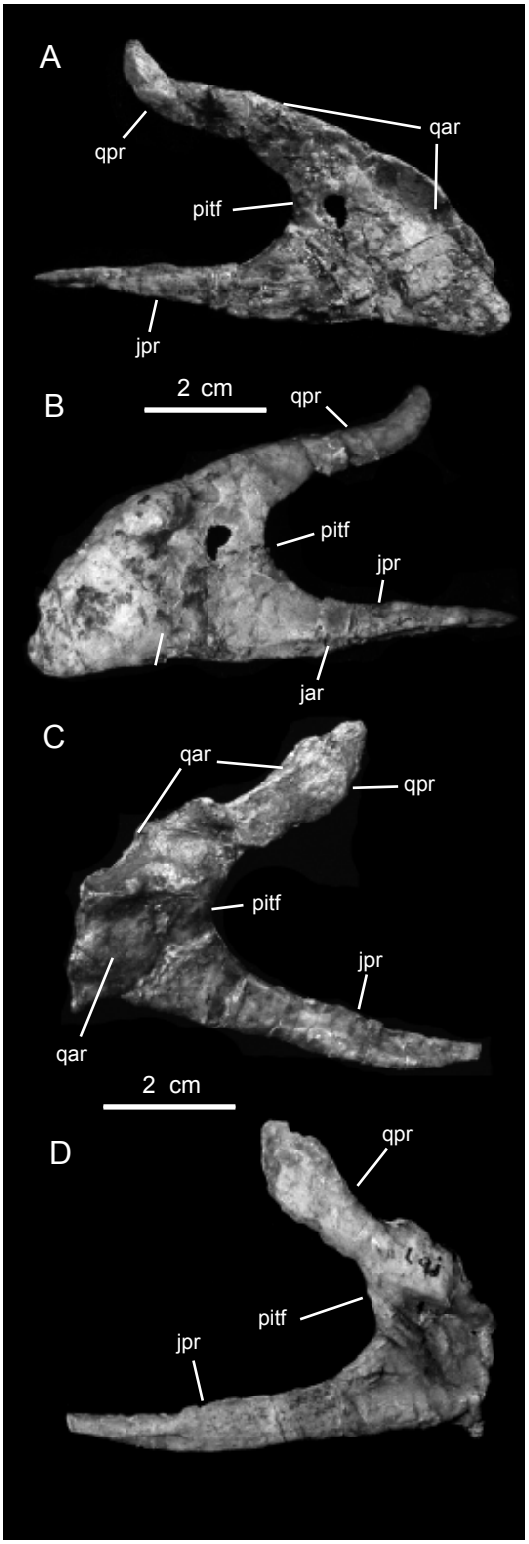

FIG. 17. Quadratojugals of *Plateosaurus erlenbergiensis* (AMNH FARB 6810). **A,** lateral and **B,** medial views of left quadratojugal. **C,** lateral and **D,** medial views of right quadratojugal. Abbreviations in appendix 2.

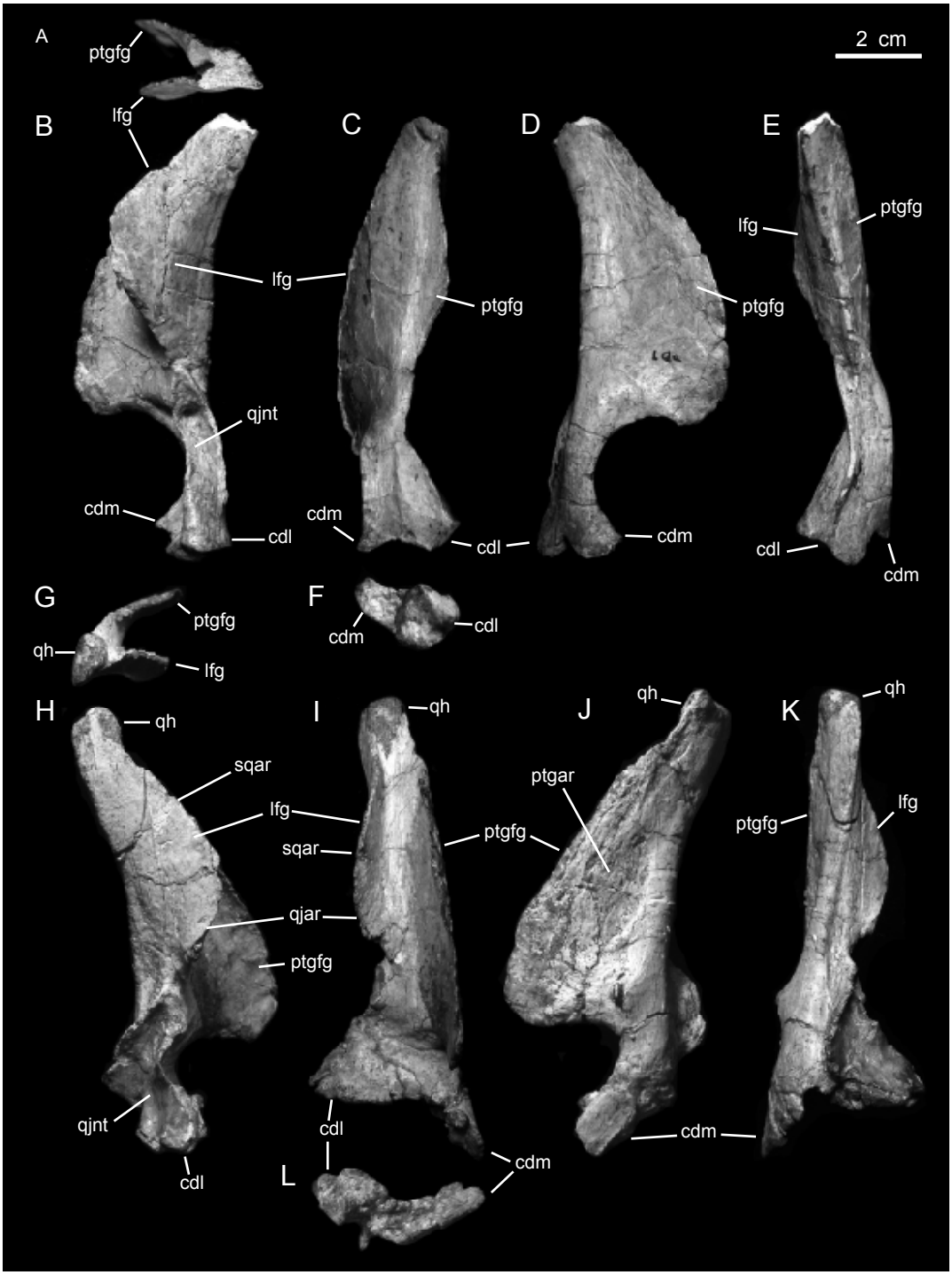

FIG. 18. Quadrates of *Plateosaurus erlenbergiensis* (AMNH FARB 6810). **A,** dorsal; **B,** lateral; **C,** anterior; **D,** medial; **E,** posterior; and **F,** ventral views of left quadrate. **G,** dorsal; **H,** lateral; **I,** anterior; **J,** medial; **K,** posterior; and **L,** ventral views of right quadrate. Abbreviations in appendix 2.

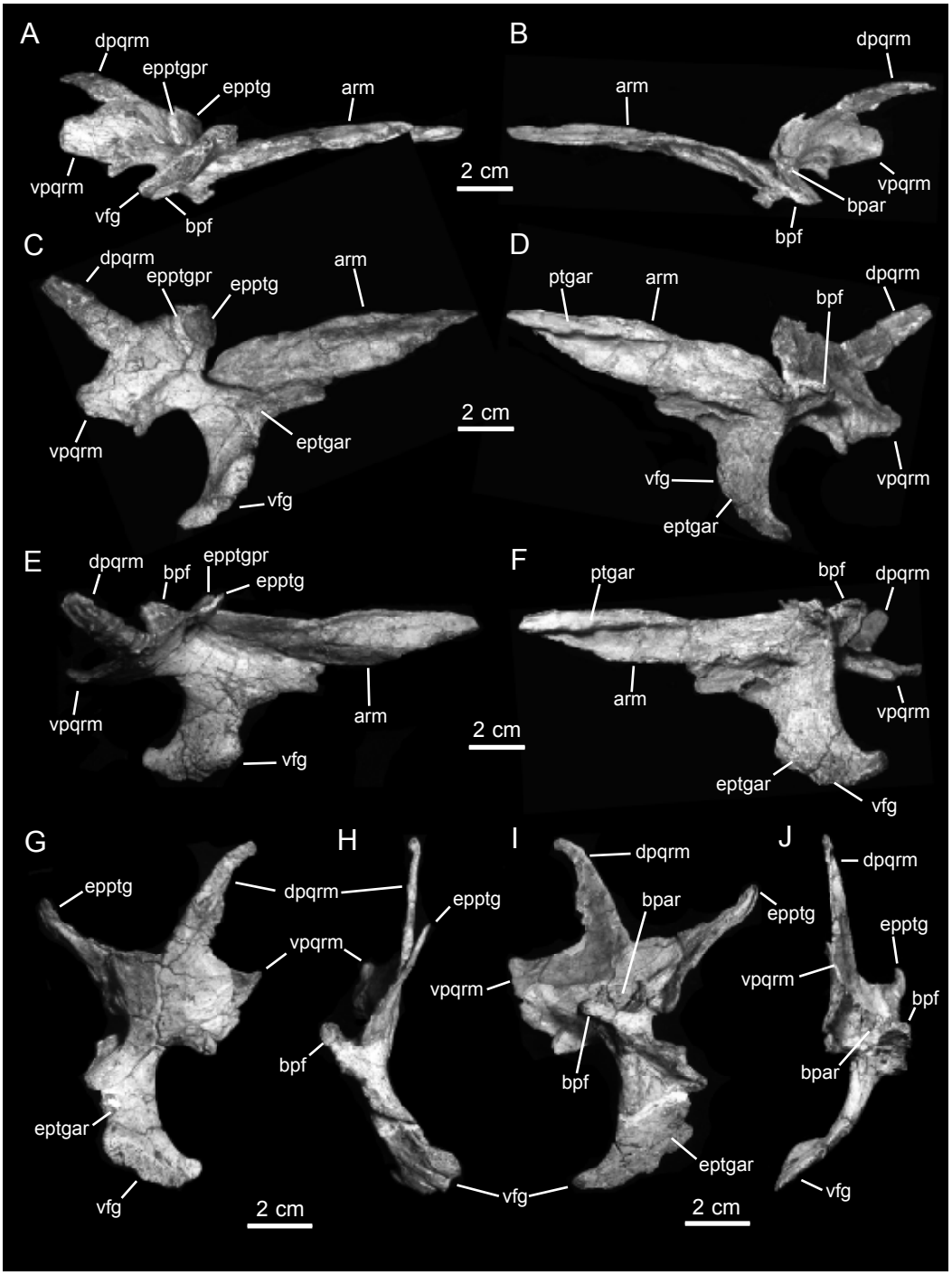

FIG. 19. Pterygoids and epipterygoid of *Plateosaurus erlenbergiensis* (AMNH FARB 6810). **A,** ventral, **B,** dorsal, **C,** lateral, **D,** medial, **E,** laterodorsal, and **F,** medioventral views of right pterygoid. **G,** lateral, **H,** anterior, **I,** medial, and **J,** posterior views of left pterygoid and epipterygoid. Abbreviations in appendix 2.

orientation to the condition seen in *Melanorosaurus readi* (Yates, 2007) and *Coloradisaurus brevis* (Bonaparte, 1978). The lateral surface of this ramus is slightly concave, as is most of the medial side. The anterodorsal orbital margin of the dorsal jugal ramus expands mediolaterally. Anteriorly and on its medial side, it is excavated by a groove that faces anteromedially and ends ventrally forming a deep pocket. This groove receives the ventral ramus of the postorbital (fig. 2). Correspondingly, the anterior and dorsal regions of the dorsal jugal ramus fit into a deeper groove in the ventral ramus of the postorbital.

The posterior ramus of the jugal is mediolaterally compressed and substantially narrower dorsoventrally than the other two rami. Like the dorsal ramus, it gradually wedges distally to a sharp point (fig. 16A, B). More than half of its length is underlain by the anterior ramus of the quadratojugal (fig. 2).

Quadratojugal: The quadratojugal is a V-shaped lamina of bone that fits in the posterolateral side of the skull between the jugal and the quadrate bones, forming the posteroventral corner of the infratemporal fenestra (figs. 2, 17). The lateral surface of the main body of the quadratojugal is laterally concave and bulges on the medial side. The medial bulge of the quadratojugal articulates with a deep and long depression on the quadrate shaft. The articulation with the quadrate extends dorsally along the dorsal ramus of the quadratojugal. The latter is a fingerlike lamina attaching to the anterior edge of the lateral wing of the quadrate (fig. 17A). The distal region of the dorsal ramus of the quadratojugal overlaps the grooved posterior border of the ventral ramus of the squamosal. The anterior ramus of the quadratojugal is straight and wedge shaped, ending in a long, sharp apex (fig. 17A, B). This ramus extends anterodorsally to overlap part of the medial surface of the posterior ramus of the jugal.

Quadrate: The quadrate is a columnar element forming the posterolateral margin of the skull, linking the latter with the mandible (fig. 2). It consists of a main shaft from which two winglike laminae project anteromedially and anterolaterally, respectively (fig. 18). The dorsal half of the shaft is mediolaterally compressed, whereas the distal half becomes more compressed anteroposteriorly and expanded mediolaterally, particularly distally (fig. 18E, K). The dorsal end of the quadrate constitutes the head, which inserts into a small ovoid socket under the posterior extreme of the squamosal (fig. 2). The quadrate head is mediolaterally compressed and triangular in dorsal view. The quadrate head is not preserved on the left quadrate.

The lateral flange of the quadrate extends along the dorsal half of the shaft and has a ventrally skewed, D-shaped profile (fig. 18B, H). The ventral half of its anterior edge articulates with the dorsal ramus of the quadratojugal, while the dorsal half meets the squamosal's ventral ramus. On the other side of quadrate, the medial flange is wider and longer than the lateral one, extending three quarters of the total length of the shaft (fig. 18D, J). Excluding its ventral margin, the medial side of this flange is occupied by a triangular depression. This depression is mostly concave ventrally and is overlapped by the posterior lamina of the pterygoid.

One the lateral side of the distal half of the quadrate shaft there is a wedge-shaped excavation. This excavation occupies the entire anteroposterior width of the shaft and deepens dorsally (fig. 18B). It is delimited by sharply defined margins. This depression receives the medial bulge of the main body of the quadratojugal.

At the distal end of the quadrate, the lateral condyle articulates into the glenoid fossa of the articular; the medial condyle articulates with the laterodorsal surface of the triangular medial process of the articular. There is a great disparity in size and width between the distal condylar regions of the left and right quadrates (fig. 18C, I). In the left quadrate, the ventral surface is slightly more than twice as wide as the lateral surface. In contrast, the ventral surface of the right quadrate is about four times wider than the lateral surface and twice as wide as that of the left quadrate. In the right quadrate the quadratojugal articular excavation is deeper and has a sharp ridge extending posteriorly from the posterolateral margin of the lateral surface of the shaft. Galton (1984) attributed these differences to a pathological distortion of the right quadrate. This would probably also explain the large morphological differences between the left and right quadratojugal (fig. 17). In the undistorted left quadrate, the lateral condyle is slightly wider anteroposteriorly than mediolaterally, and almost heart shaped in contour (fig. 18F). In contrast, the medial condyle is mediolaterally elongate and subtriangular. The ventral surface of the medial condyle is concave, whereas that of lateral condyle is irregularly textured. The lateral condyle is larger and ventrally offset slightly relative to the medial one. In contrast, the right quadrate of AMNH FARB 6810 and the quadrates of *Riojasaurus incertus* (Bonaparte and Pumares, 1995) and *Yunnnanosaurus huangi* (Barrett et al., 2007) have the medial condyle more ventrally positioned than the lateral one. The slight ventral projection of the medial condyle in the left quadrate of AMNH FARB 6810 and the observed texture of both condyles may be due to the lack of preservation of a cartilaginous cap that, as indicated by Galton (1984), might have completed the condylar surface of the quadrate.

Palate

Pterygoid: The pterygoid is the largest element of the palate and forms the posterior half of the palatal complex. It is composed of three large rami and a short process projecting from a reduced and dorsoventrally constricted central body (fig. 19). The three major rami are the anterior palatal ramus, the posterolateral quadrate wing, and the lateroventral flange. The right pterygoid is nearly completely preserved, missing the distal end of the dorsal process of the quadrate wing (fig. 19A–F). In contrast, the left pterygoid preserves only most of the hooklike sheet of the lateroventral flange and the main body of the quadrate wing (fig. 19G–J).

The anterior palatal ramus is the longest structure of the pterygoid and projects anteriorly and slightly dorsally. This ramus consists of a mediolaterally compressed lamina and is roughly lanceolate in lateral view and tapers anteriorly to a sharp apex (fig. 19C). A deep groove on the laterodorsal surface of the pterygoid separates the proximal half of the anterior ramus from the quadrate wing and the lateroventral flange. This groove results in an anteroposteriorly elongate bulge on the bone's medial surface. The lateral surface of the proximal half of the ramus is flat, whereas the medial surface is gently concave. The lateral surface of this distal segment of the anterior ramus is strongly convex dorsoventrally and the medial surface is deeply excavated. Dorsal and adjacent to this excavation, the dorsal border of the medial side of this ramus is offset medially and forms a narrow and slightly grooved facet that continues into the pointed apex of the ramus (fig. 19D). This grooved facet represents the contact of the anterior rami of

both pterygoids. The ventral margin of the proximal half of the anterior ramus is continuous ventrally with the proximal base of the lateroventral flange.

The lateroventral flange of the pterygoid is composed of an anteroposteriorly broad and dorsoventrally compressed proximal base and a posteroventrally curving hook-shaped process (fig. 19C–F). The semicircular lateroventral border of this process is thick, particularly along its anterior area that overlaps the posteroventral margin of the ectopterygoid (fig. 20A, D). When articulated, the ventral margin of the proximal base of the lateroventral flange of the pterygoid, lying between the hook-shaped process and the anterior ramus (fig. 19C), is overlapped by the medial flange of the ectopterygoid (fig. 20C).

The quadrate wing is a broad lamina projecting posterodorsally and gently curving laterally from the central body of the pterygoid (fig. 19C, D). Its proximal end is dorsoventrally constricted, forming a necklike base merging with the central body of the pterygoid. As it expands dorsoventrally, the quadrate wing bifurcates posteriorly into two processes, which articulate with the quadrate's pterygoid wing. The ventral process is subtriangular, relatively short, and projects ventrally to abut against a recess near the posterior border of the medial side of the pterygoid wing of the quadrate. The dorsal process is long and wedge shaped, projecting posterodorsally and tapering gradually into a narrow apex. The entire lateral surface of this process attaches to the anterodorsal border of the medial surface of the pterygoid wing of the quadrate.

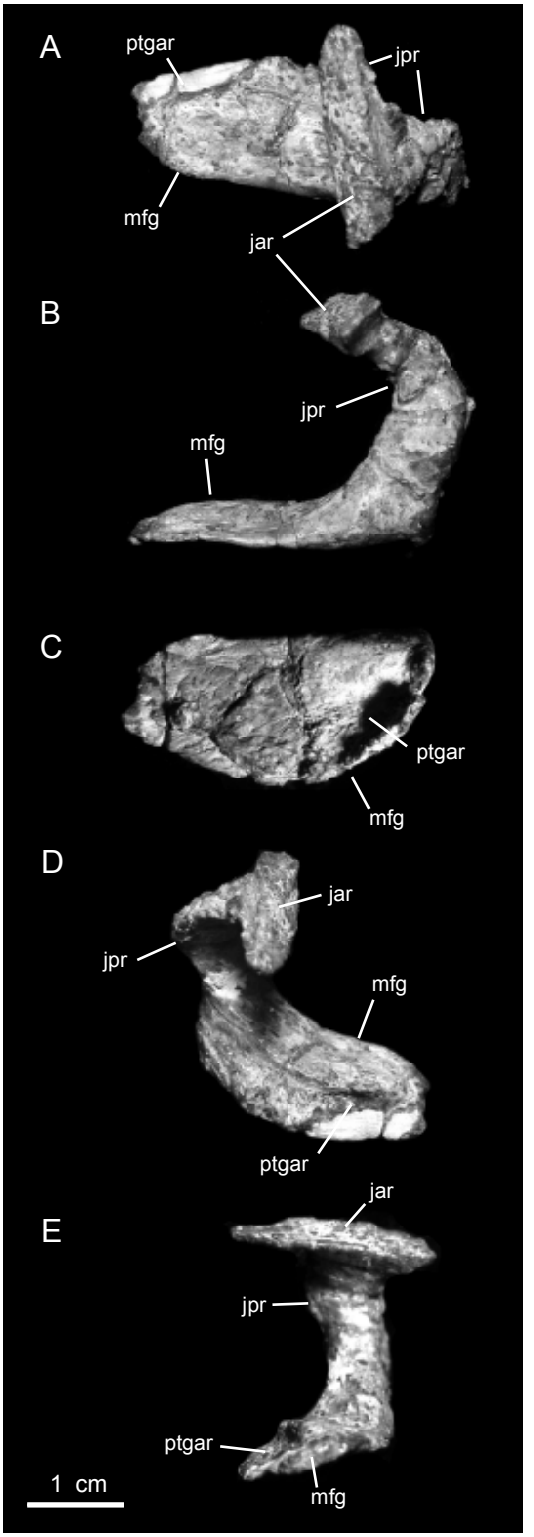

FIG. 20. Right ectopterygoid of *Plateosaurus erlenbergiensis* (AMNH FARB 6810). **A,** lateral; **B,** anterior; **C,** medial; **D,** posterolateral; **E,** ventral. Abbreviations in appendix 2.

A short flange projects posteromedially from the medial side of the central body of the pterygoid (fig. 19B–F), medial to the region where the anterior ramus, the quadrate wing, and the lateroventral flange converge. This flange articulates with the basipterygoid process of the basisphenoid.

Epipterygoid: The epipterygoid consists of a simple elongate and mediolaterally compressed bony projection attaching to the lateral surface of the anterodorsal region of the quadrate wing of the right pterygoid (fig. 19C, G, I). The epipterygoid projects anterodorsally and tapers distally to articulate with a deep concavity on the anteroventral surface of the laterosphenoid.

Ectopterygoid: The ectopterygoid is a U-shaped element that connects the palatal complex with the rostral facial skeleton. It is composed of a slightly curved, rodlike, short shaft that expands at both ends (figs. 20, 21). In the right ectopterygoid, the medial segment of the shaft is strongly recurved and slightly twisted as a consequence of postdepositional distortion (fig. 20). The medial end of the ectopterygoid is dorsoventrally (and slightly anteroposteriorly) expanded into a broad flange. The medial aspect of this flange is slightly concave (more so dorsally) (figs. 20C, 21C) and overlaps the ventral margin of the proximal region of the lateroventral flange of the pterygoid. The posterior margin of the lateral surface of the medial flange of the ectopterygoid contains an elongate recess (fig. 20A, D) that underlies the anteroventral corner of the hooklike process of the lateroventral flange of the pterygoid.

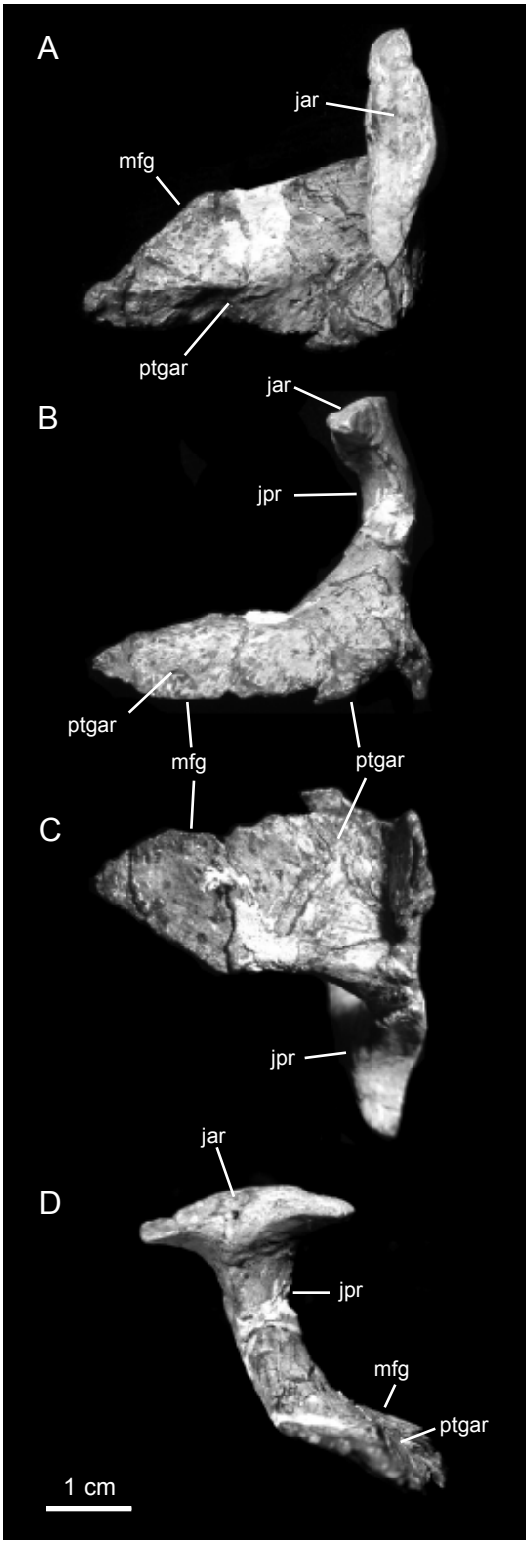

FIG. 21. Left ectopterygoid of *Plateosaurus erlenbergiensis* (AMNH FARB 6810). **A,** lateral; **B,** posterior; **C,** medial; **D,** ventral. Abbreviations in appendix 2.

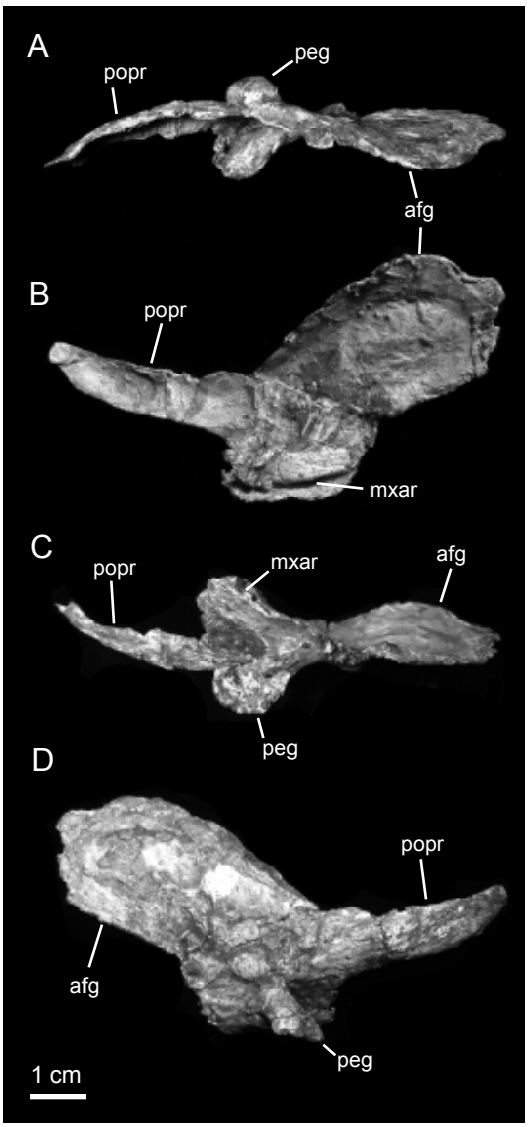

FIG. 22. Right palatine of *Plateosaurus erlenbergiensis* (AMNH FARB 6810). **A,** ventral; **B,** lateral; **C,** dorsal; **D,** medial. Abbreviations in appendix 2.

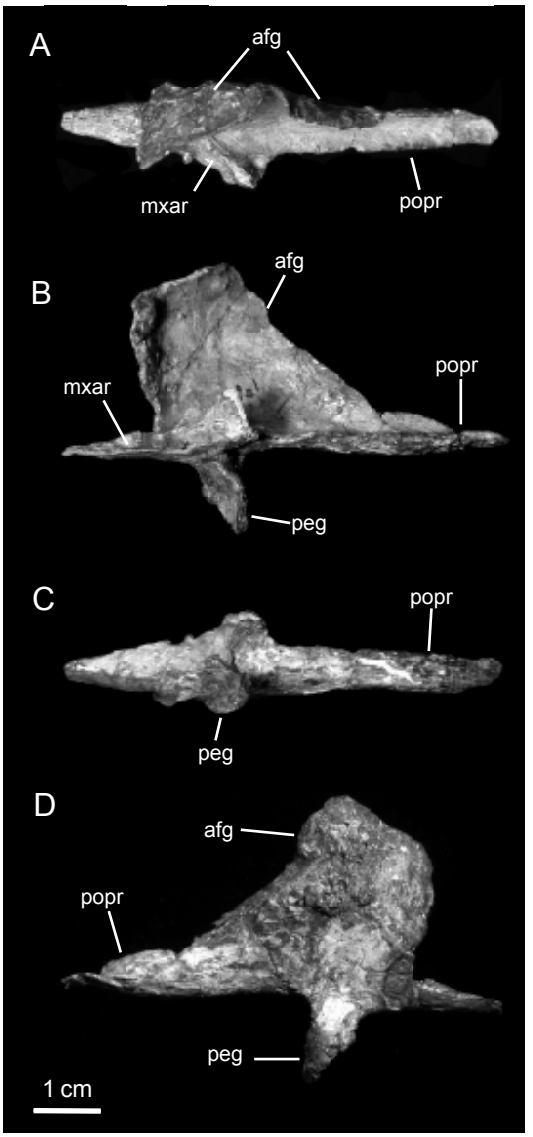

FIG. 23. Left palatine of *Plateosaurus erlenbergiensis* (AMNH FARB 6810). **A,** ventral; **B,** lateral; **C,** dorsal; **D,** medial. Abbreviations in appendix 2.

At the other end of the shaft lies the lateral process. The left element has been heavily reconstructed. On the right ectopterygid, which is well preserved, this process expands anteroposteriorly, forming a T-shaped dorsal and ventral profile with the lateral half of the shaft (fig. 21D). The lateral surface of the expansion is flat and D-shaped. It articulates with an arcuate groove on the medioventral side of the jugal.

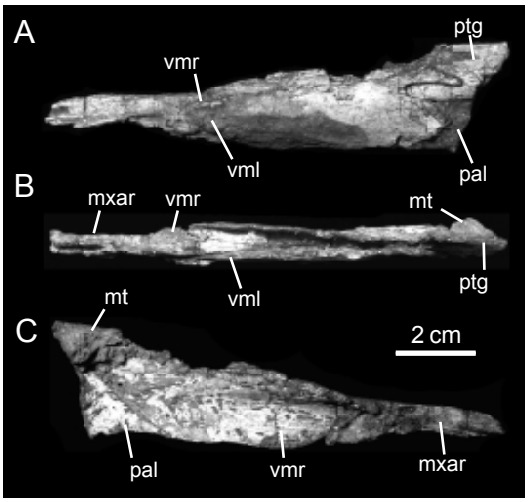

FIG. 24. Vomers (with anterior ends of palatine and pterygoid) of *Plateosaurus erlenbergiensis* (AMNH FARB 6810). Abbreviations in appendix 2. **A,** left vomer in lateral view. **B,** left and right vomer in dorsal view. **C,** right vomer in lateral view. Abbreviations in appendix 2.

Palatine: This element consists of a thin lamina that forms an anterodorsally projecting flange and two elongate processes that project posteriorly and anteriorly from the base of the flange (figs. 22, 23). The anterodorsal flange is tilted slightly medially and is slightly broader distally. The lateral surface of the flange is gently concave near the dorsal and anterodorsal margins. It contacts the anterior ramus of the pterygoid (Galton, 1984). The anterior palatine process is only partially preserved in the left element of AMNH FARB 6810 (fig. 23) and a small fragment is preserved attached to the lateral surface of the left vomer (fig. 24C). The anterior process is extremely compressed dorsoventrally and tapers anteriorly. Its ventral surface is gently convex transversely. In contrast, its dorsal surface is slightly concave and underlies the palatine flange on the medial side of the posterior ramus of the maxilla (fig. 4B). Posteriorly, toward the center of the base of the palatine, the anterior process is continuous with a short and thick ridge forming a prominent posteromedial projection (fig. 23A, B). A flange extends medially below this ridge from the base of the anterodorsal lamina of the palatine. A narrow groove is present between the oblique ridge and the medial flange (figs. 22B, 23A) for reception of the palatine ridge on the posterior ramus of the maxilla's medial surface.

A short and anteroposteriorly compressed peglike process projects ventromedially and slightly posteriorly from the ventral surface of the palatine (figs. 22D, 23B). This process is constricted proximally and shows a concave anterolateral surface and a convex posteromedial surface. The presence of this peglike process is autapomorphic to *Plateosaurus erlenbergiensis* (Galton and Upchurch, 2004). The posterior process of the palatine is more completely preserved in the right palatine, where it is as long as the anterodorsal flange (fig. 22B). The process shows a deeply concave laterodorsal surface and a convex medioventral side. According to Galton (1984), this process articulates with the ectopterygoid and the ventral region of the ventral flange of the pterygoid.

Vomer: The vomer is narrow and anteroposteriorly elongate and forms the anterior region of the palate (fig. 24). The left and right vomers are partially preserved in AMNH FARB 6810. Small fragments (which were probably broken during disarticulation of the skull) of the palatine and pterygoid are attached to the posterior parts of the vomers (fig. 24A, C). The tapering anterior end of each vomer shows a narrow and grooved lateral surface for articulation with the vomeral flange present on the medial surface of the anterior end of the maxilla (fig. 4B).

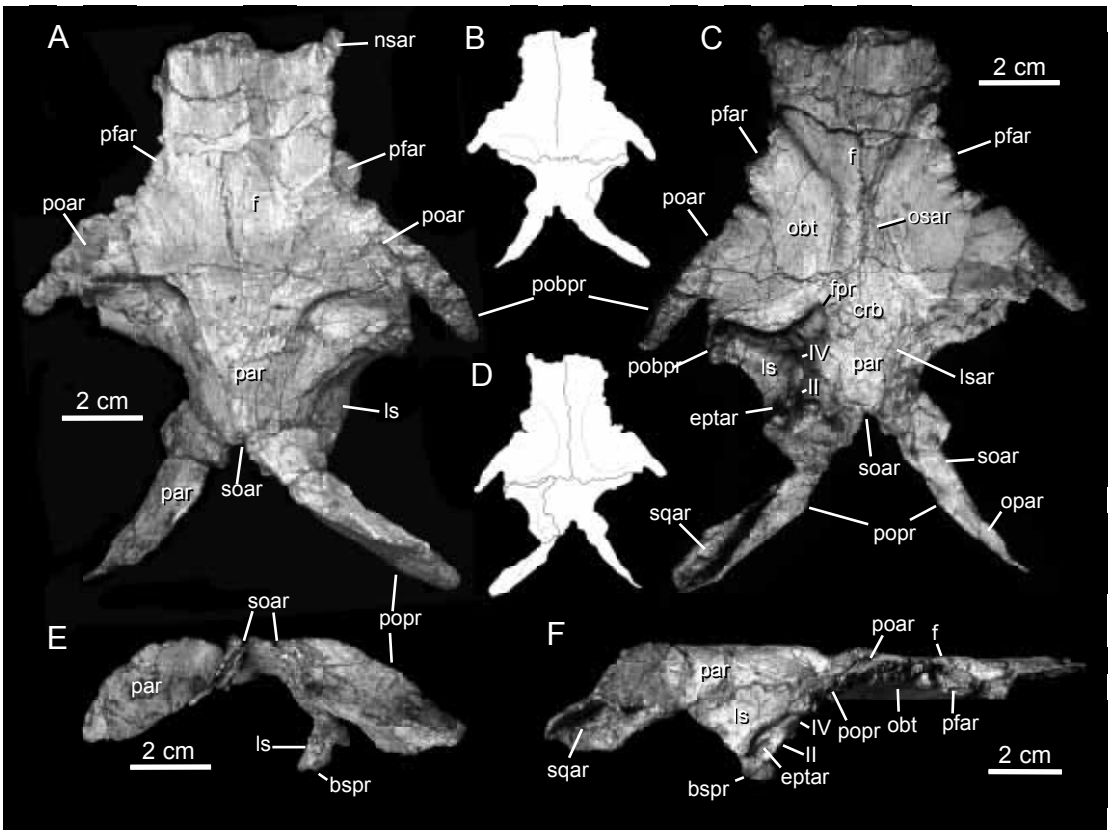

FIG. 25. Skull roof (frontal, parietal and right laterosphenoid) of *Plateosaurus erlenbergiensis* (AMNH FARB 6810). **A,** lateral and **B,** medial views of right sclerotic ring. **C,** lateral and **D,** medial views of left sclerotic ring. Abbreviations in appendix 2.

Neurocranium

Frontal: The paired frontals are large and thick bone sheets roofing the skull dorsolateral and posterior to the orbits. The anterior half of each frontal (anterior to the articulation with the postorbital) is rectangular in dorsal view, whereas the posterior half (lateral to the postorbital) is greatly expanded mediolaterally (fig. 25A). The anteriormost region of the frontal is the thinnest area of the bone. The articulation with the nasal occurred along the anterior margin of the frontal. However, it is incompletely preserved in AMNH FARB 6810, lacking the border that would be overlapped by the nasal anteriorly and by the dorsal flange of the prefrontal laterally. The lateral margin of the anterior half of the frontal is crenulated and dorsoventrally expanded. This margin articulates with the medial side of the dorsal flange of the prefrontal. A small portion of the frontal between the postorbital and prefrontal articular margins contributes to the dorsal rim of the orbit.

The dorsal surface of the rectangular anterior half of the frontal is slightly concave transversely, with a gently elevated medial border at the interfrontal suture. The dorsal surface of the posterior half of the frontal is anteriorly gently domed. Posteromedial to the articulation

with the postorbital, the dorsal surface of each frontal shows a deep and oval excavation (fig. 25A) with a long mediolaterally oriented axis. The anterior and medial margins of this excavation form an arched and sharp edge elevated dorsally relative to the posterior and lateral surfaces of the excavation. This sharp margin is continuous with a similar edge on the posteromedial side of the anterior ramus of the postorbital. When the frontal and postorbital articulate, these sharp margins form the anterior boundary of the supratemporal fenestra.

The articular surface for the postorbital lies anterior and lateral to the posterolateral excavation of the frontal. In that area, the lateral margin of the frontal is thick dorsoventrally and very irregular in texture. It faces anterolaterally rather than laterally. A narrow and rugose surface separates this margin from a fingerlike postorbital process. This process is dorsoventrally compressed and projects posterolaterally forming an angle of 140° relative to the sagittal plane of the skull (fig. 25A, B). The process is as long as the combined mediolateral width of the anterior half of both frontals. It inserts into a groove on the ventral surface of the anterior ramus of the postorbital. Correspondingly, the dorsal surface of the anterior ramus of the postorbital overlaps the dorsal surface of the fingerlike process and the rugose dorsal surface of lateral margin of the frontal that lies just posterior to the process. The articulation with the parietal is a transverse interdigitating suture (fig. 25A) and the interfrontal suture is very thin and slightly sinuous.

The ventral side of both articulated frontals display an hourglass-shaped recessed surface encased between the semicircular orbital

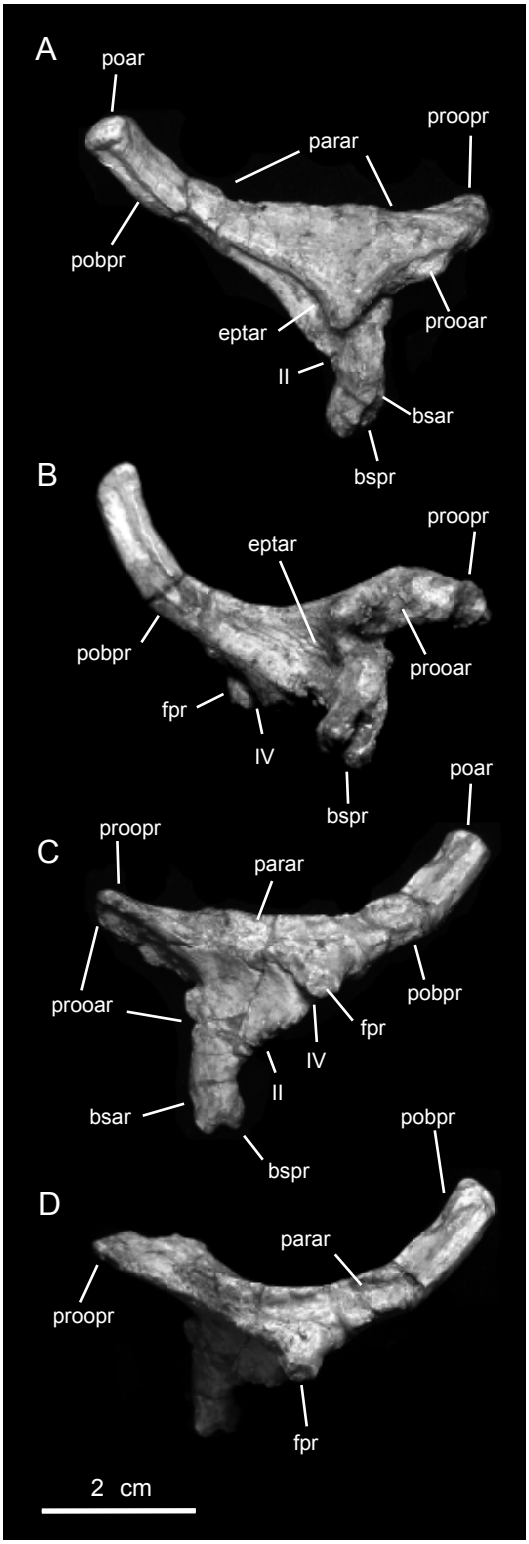

FIG. 26. Left laterosphenoid of *Plateosaurus erlenbergiensis* (AMNH FARB 6810). **A,** lateral; **B,** ventral; **C,** medial; **D,** dorsal. Abbreviations in appendix 2.

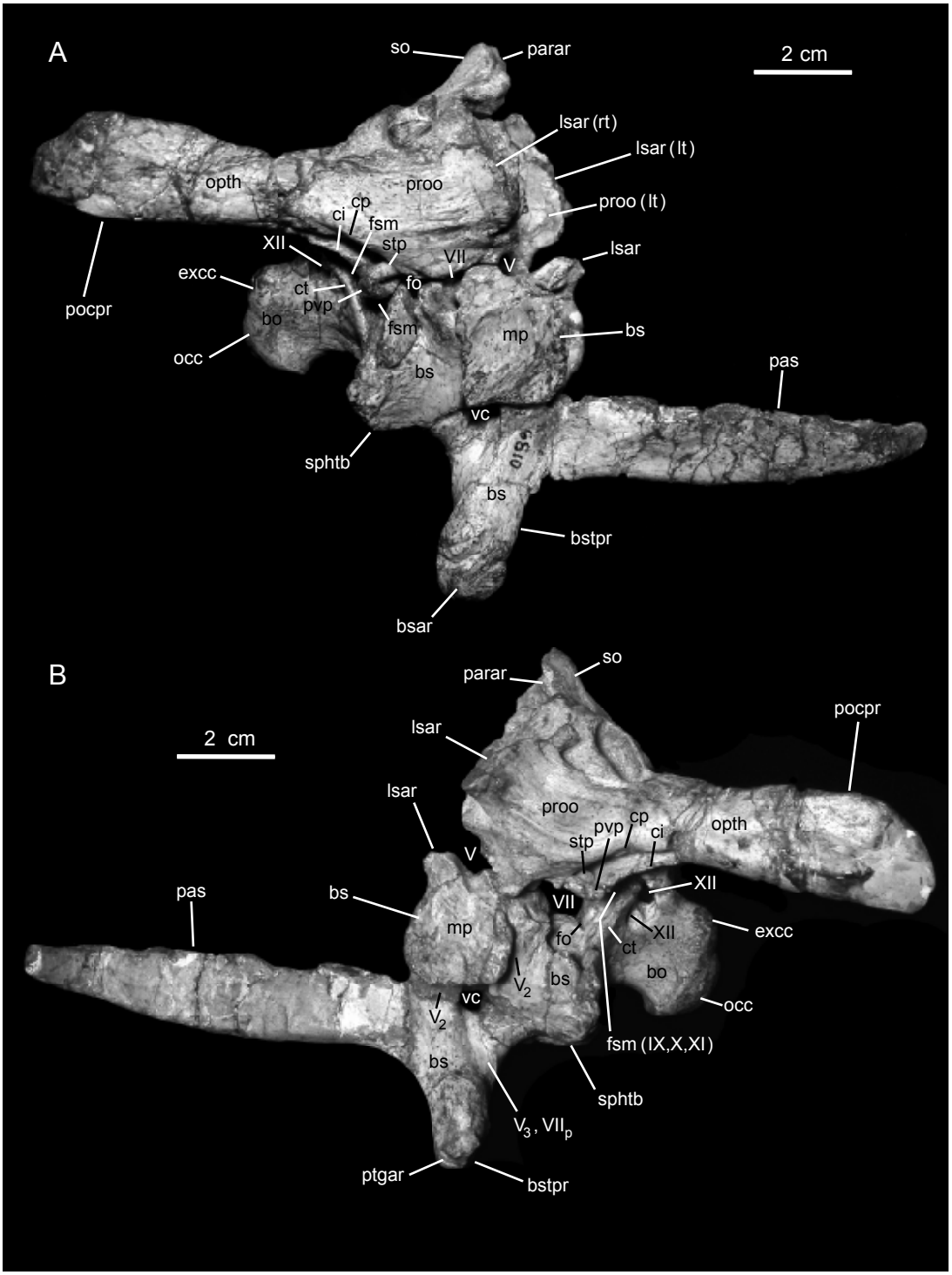

FIG. 27. Braincase of *Plateosaurus erlenbergiensis* (AMNH FARB 6810). **A,** right lateral; **B,** left lateral. Abbreviations in appendix 2.

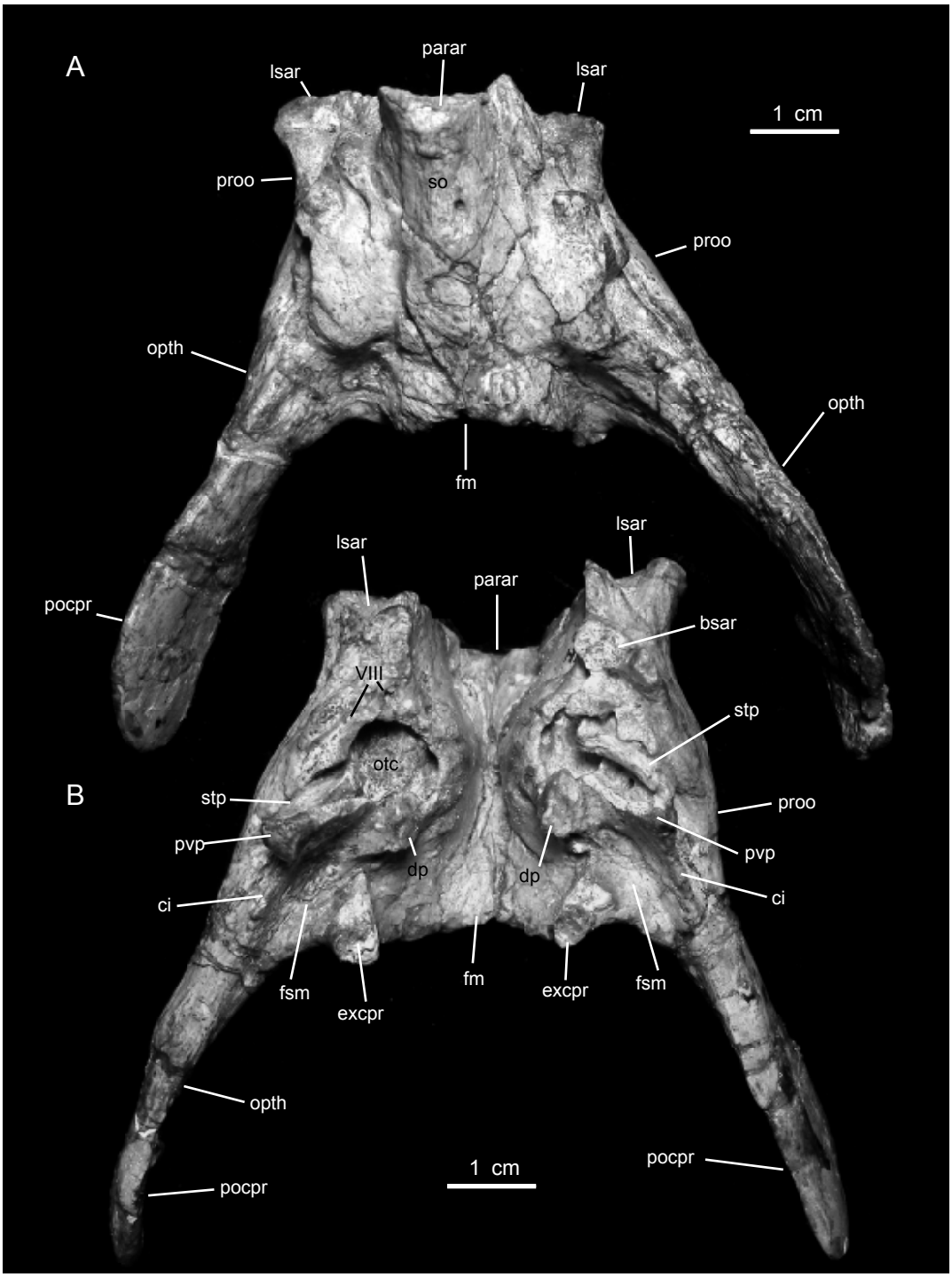

FIG. 28. Dorsal region (opisthotic, supraoccipital, prootic, laterosphenoid) of the braincase of *Plateosaurus erlenbergiensis* (AMNH FARB 6810). **A,** dorsal; **B,** ventral. Abbreviations in appendix 2.Abbreviations in appendix 2.

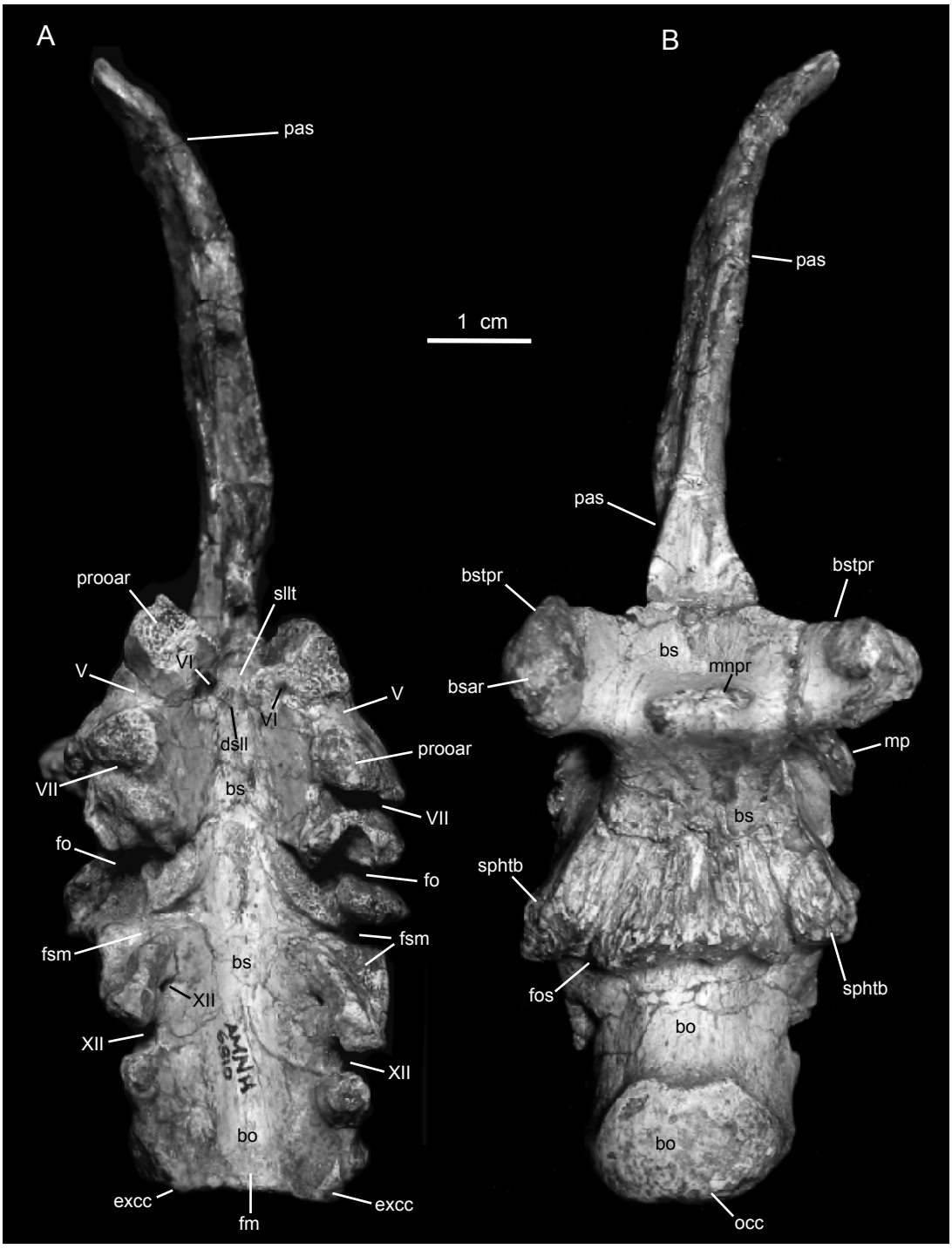

FIG. 29. Ventral region (exoccipital, basioccipital, basisphenoid, parasphenoid) of the braincase of *Plateosaurus erlenbergiensis* (AMNH FARB 6810). **A,** dorsal; **B,** ventral. Abbreviations in appendix 2.

regions (fig. 25B). This morphology is also present in *Massospondylus kaalae* (Barrett, 2009: fig. 4B). The anterior region of the "hourglass" surface in AMNH FARB 6810 is subtriangular and sculpted with longitudinal striations. Posteriorly, it narrows abruptly into the groovelike olfactory depression. Posteriorly, the olfactory surface opens into the deeper cerebral cavity, most of which is formed by the parietal. This cavity is suboval in ventral profile and is slightly longer anteroposteriorly than mediolaterally (fig. 25B). Lateral to the olfactory and cerebral cavities, the two orbital surfaces display a smooth texture. Each of these orbital regions is rather flat medially, becoming gently concave anteroposteriorly near the lateral margin of the frontal. The medial margin of the orbital surface is thick and sharply defined. Its posterior margin articulates with the laterosphenoid (fig. 25B).

Parietal: In dorsal view, the parietal is an anteroposteriorly abbreviated hourglass-shaped element (fig. 25A). Anteriorly, the parietal is greatly expanded into a pair of anterolateral processes. The anterior edge of the parietal contains the interdigitating suture with the frontals. The width across the anterolateral processes is about two and a half times longer than the main body of the parietal at its minimum breadth. Most of the dorsal surface of the parietal is flat, except for the concave lateral regions. Sagittally, there is a relatively wide and very low, smooth ridge. The ventral surface of the parietal is deeply concave, forming most of the roof and part of the lateral wall of the cerebral cavity.

The posterior region of the parietal consists of two large "hornlike" processes (fig. 25). These processes diverge and project posterolaterally. The long axis of each process forms an angle of about 45° to the sagittal plane of the skull. Each process is about 1.8 times as long as the rest of the parietal. The processes are mediolaterally compressed and dorsoventrally broad. The dorsal edge of the proximal three quarters of these processes bear large and thin flanges. Proximally, this flange is continuous with a sharp but faint line laterally located to the low sagittal ridge of the parietal. The space that exists between the proximal segment of the posterolateral processes receives the anterodorsal and anterolateral regions of the supraoccipital. Posteriorly, a sharp and prominent medial ridge of each one of the posterolateral processes of the parietal articulate with the lateral region of the opistothic-exoccipital complex.

Basioccipital: The basioccipital is cup-shaped element and forms the posterior half of the floor of the braincase, most of the occipital condyle (its laterodorsal corners are formed by the exoccipital), and probably the posterior parts of the sphenooccipital tubera (figs. 27, 29, 30). The occipital condyle lies above the level of the parasphenoid (fig. 27), which, according to Galton (1990), is diagnostic of *Plateosaurus engelhardti* (herein an autapomorphy for *P. erlenbergiensis*, see below). The condyle is hemispherical and heart shaped in posterior view. Its smooth ventral surface is convex mediolaterally and, to a lesser degree, anteroposteriorly. The posterior surface of the condyle is flat and tilts slightly anteriorly. Near the center of this surface there is a small, shallow circular depression. The dorsal margin of the occipital condyle constituting the ventral edge of the foramen magnum is sharply defined. Anterior and adjacent to this edge, the dorsal surface of the basioccipital forms a trench that has a V-shaped cross section and is anteriorly continuous with the basisphenoid to form the floor of the braincase (fig. 29A). Anteriorly, at the basioccipital-basisphenoid joint, the ventral surface of the basioc-

cipital curves ventrally becoming oriented vertically. At the center of this vertical surface there is a deep circular depression, just dorsal and adjacent to the posterodorsal margin of the sphenooccipital tuber. Immediately posterior to the latter, the basioccipital shows a pair of oval fossae delimited by sharply defined edges (figs. 29B, 30B).

Basisphenoid: The basisphenoid forms the anterior half of the floor of the braincase and its dorsal margin forms the ventral half of various neurocranial foramina (figs. 27, 29). These are, from anterior to posterior, the trigeminal foramen, the facial foramen, the fenestra ovalis (= vestibuli), and the anterior half of the fissura metotica. The basisphenoid can be divided into three parts, consisting of the posterior, anterodorsal, and anteroventral regions. The external opening of the vidian canal lies at the juncture of these three regions (fig. 27A). The posterior region of the basisphenoid is composed of its posterolateral wall and, ventrally, of most of the sphenoccipital tubercles (or basal tuberae). Anterior to posterolateral wall of the element and dorsal to the pterygoid processes, the anterodorsal region of the basisphenoid encloses the sella turcica. The anteroventral region of the basisphenoid is composed primarily of the pterygoid processes. The latter are separated from the sphenoccipital tubercles by a "neck-shaped" mediolateral constriction. The dorsal surface of the basisphenoid consists of a deep and wide channellike surface (fig. 29A).

On the ventral surface of the basisphenoid, the sphenoccipital tubercles radiate into four projections separated by narrow grooves (fig. 29B). The median groove is teardrop shaped, as well as the widest and deepest. The ventral surfaces of the sphenoccipital tubercles are flat and sculpted with coarse longitudinal striations that attenuate anteriorly. The posterior margins of the tubercles are cup shaped, very rugose in texture, and are part of the basioccipital. A transverse crenulated suture between the latter element and the basisphenoid is present on the ventral surface of the tubercles. The lateral surface of the posterior wall of the basisphenoid dorsal to the tubercles is flat and faces anterolateraly. Near its dorsal border, this surface becomes concave to form the ventral region of the fenestra ovalis.

The anterior third of the basisphenoid encloses the sella turcica anteriorly and the anterodorsal opening of the vidian canal posteriorly. The sella turcica is a deep cavity that shows a diamond-shaped profile in anterior view. The lateral surface of anterior third of the basisphenoid serves as the attachment site for the M. protractor pterygoideus (Galton, 1984; Benton et al., 2000). This surface is rectangular, flat, smooth, and faces anterolaterally, forming a 25° relative to the sagittal plane of the braincase (figs. 27, 29). It is bounded by well-defined edges and is slightly offset laterally relative to the posterior region of the basisphenoid. This offset allows this lateral surface of the anterior region of the basisphenoid to slightly overlap the lateral surface of the posterior region.

The ventral region of the basisphenoid is composed primarily of the basipterygoid processes (figs. 27, 29B). Bordering ventrally the vidian canal, the lateral surface of the basisphenoid is concave dorsoventrally, facing laterodorsally and slopping lateroventrally. This sloping surface is smooth and continuous with the proximal surface of the basipterygoid process. Ventral and adjacent to the vidian canal, the bone surface is slightly recessed and separated from the proximal segment of the basipterygoid process by a faint ridge. The posterior side of the

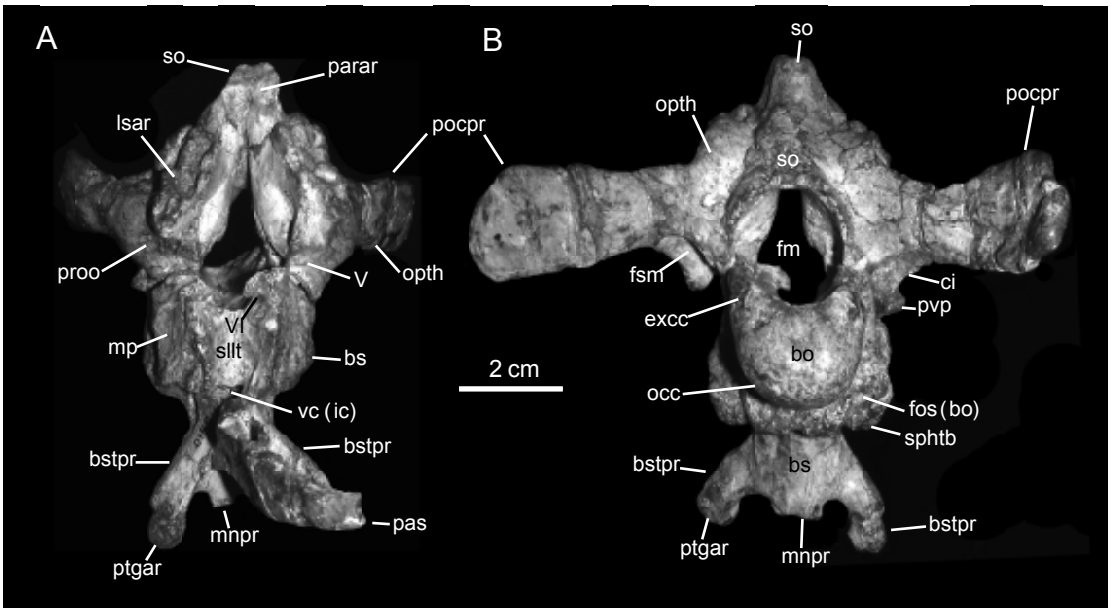

FIG. 30. Braincase of *Plateosaurus erlenbergiensis* (AMNH FARB 6810). **A,** anterior; **B,** posterior. Abbreviations in appendix 2.

ventral region of the basisphenoid is flat and vertical, connecting dorsally with the sphenooccipital tubercles (fig. 29B). The basipterygoid processes project anteroventrally, forming an angle of 60° between their long axes. Proximally, these processes are moderately compressed mediolaterally and distally they separate substantially. The anterior margin of each basipterygoid process, between the contact with the parasphenoid and its distal end, is narrow and sharply defined. The distal end of each process is rounded and moderately expanded as it contacts the basipterygoid flange lying on the medial side of the central region of the pterygoid (fig. 19D, F). The anterior surface of the basisphenoid that lies between the basipterygoid processes is smooth, triangular, and concave (fig. 29B). Dorsally, this anterior surface is bounded by the posterior margin of a deep cavity of the proximal end of the parasphenoid. Ventrally, the posteroventral margin of the anterior surface present between the pterygoid processes forms a transverse thick ridge. At the center of this ridge there is a short and rectangular median process. This process projects ventrally a few millimeters from the transverse ridge (figs. 29B, 30B).

Parasphenoid: The parasphenoid is mediolaterally compressed and elongate. It projects forward from the anterior surface of the basisphenoid, just below the sella turcica and above the basipterygoid processes (figs. 27, 29). The parasphenoid is about 28% longer than the combined anteroposterior length of the basioccipital and basisphenoid. The dorsal and ventral margins of the proximal half of the parasphenoid are subparallel. Further distally, these margins gradually converge at their apex. The ventral side of the proximalmost region of the parasphenoid, adjacent to the anterodorsal fossa that lies between the basipterygoid processes of the basisphenoid, contains a triangular excavation delimited by sharp margins. Anterior to this

excavation, the ventral side of the parasphenoid narrows abruptly mediolaterally to form the ventral edge of the element. In contrast, the mediolateral narrowing of the dorsal surface of the parasphenoid occurs more gradually than the ventral margin. Only the distal third of the dorsal margin of the parasphenoid is as narrow as the ventral margin.

Laterosphenoid: The laterosphenoid is a mediolaterally compressed element contributing to the anterior region of the lateral wall of the braincase (figs. 25, 26). It articulates with the prootic posteriorly, the opisthotic posterodorsally, and the basisphenoid ventrally. The lateral surface of the laterosphenoid is slightly concave anteroposteriorly and continuous with the lateral surface of the parietal ventral to the supratemporal fenestra. The ventral margin of the lateral surface projects as a triangular apex (fig. 26A). The medial surface is also gently concave, both anteroposteriorly and dorsoventrally. A notch on the sharp anteromedial edge of the laterosphenoid probably formed part of the foramen for the optic nerve. Another, less well-defined notch, bounded dorsomedially by the frontal process, is found dorsal to that for the optic nerve and probably represents the posterodorsal margin of the trochlear nerve foramen (figs. 25C, F, and 26).

Anteriorly, the laterosphenoid becomes mediolaterally expanded and bifurcates into the anterolateral postorbital process and the frontal process anteromedially (fig. 25C). The dorsal margins of these processes, as well as that of the more posterior body of the laterosphenoid, fit into wide grooves on the ventral surface of the frontal and parietal. The anterolateral process of the laterosphenoid arches laterally and anteriorly, while projecting slightly dorsally to fit into a subrectangular depression on the medial surface of the proximal region of the anterior ramus of the postorbital. In the disarticulated right laterosphenoid the distal segment of this postorbital process has been reconstructed (fig. 26). The anteromedial process is shorter and narrower than the anterolateral postorbital process (fig. 25C) and contacts the frontal anteriorly. It is subcylindrical projection and borders the posterior margin of the orbital surface of the frontal. This anteromedial frontal process is nearly completely preserved in the articulated left laterosphenoid; only the proximal end is preserved in the right laterosphenoid (fig. 26C).

The broad anteroventral border of the laterosphenoid contains a longitudinal groove extending anteriorly into the ventral surface of the anterolateral process. Posteriorly, this groove contains a deep oval depression for reception of the dorsal end of the epipterygoid (figs. 25F, 26A). Posterior to this depression lies the basisphenoid process, which projects ventrally to meet the basisphenoid and is medially recessed relative to the triangular ventral projection on the lateral surface of the laterosphenoid (fig. 26A).

Prootic: The prootic occupies a central part of the lateral braincase wall, posterior to the laterosphenoid and anterior to the opisthotic-exoccipital complex (figs. 27, 28). The prootic overlaps anteriorly the posterolateral surface of the laterosphenoid. Posteriorly, it wedges into a narrow apex that overlaps the lateral surface of the anterior region of the opisthotic-exoccipital complex. The posterior margin of the foramen prooticum for the trigeminal nerve is formed by the prootic, whereas the anterior margin is formed by the laterosphenoid. Just dorsal to the dorsomedial corner of the sella turcica there is a foramen that transmitted cranial nerve VI—the abducens (figs. 29A, 30A). The dorsal boundary of this foramen is composed of a curved

bridgelike structure formed by medial prolongation of the anteromedial margin of the ventral region of the basisphenoid (fig. 30).

The lateral surface of the prootic is anteroposteriorly concave and has a series of longitudinal striations and fine ridges (fig. 27B). The latter are more numerous within the ventral third of the bone where there is a deep and elongate excavation. Ventral to this excavation the prootic forms the dorsal margin of the foramen for the facial nerve (CN VII). Anteroventral to the crista prootica, the prootic forms the dorsal border of the fenestra ovalis. The crista prootica and the crista interfenestralis enclose an oblique cavity that curves dorsally and posteriorly underlying the base of the paroccipital process and lying adjacent to the otic capsule. The roof of this oblique cavity contains the suture between the opisthotic and the posterior wedge of the prootic (fig. 28B). Both stapes are preserved, having collapsed into the vestibular cavities at each side of the braincase (fig. 28B). These are columnar and proportionately robust elements. Each stapes is slightly compressed mediolaterally and moderately expanded at its medial end to form the footplate. The footplate has a subsquared contour and has a flat surface. Adjacent and posterior to that oblique cavity is the fissura metotica. Its anterior wall is composed of the crista interfenestralis, while its posterior wall is formed by the crista tuberalis. Ventrally, the crista interfenestralis expands to form a relatively large flange. This flange is most expanded anteroposteriorly and is mediolaterally thicker at its lateral end. Similarly, the ventral end of the crista tuberalis is particularly thick where it merges with the lateral edge of the foramen magnum, just above the occipital condyle. Galton (1984) reported a divided fissura metotica, composed of a foramen lacerum posterior dorsomedially and a foramen jugular medioventrally. However, our reexamination of the fissura metotica indicates that it is actually undivided and that the apparent division is due to the presence of a well-developed descending process of the opisthotic, which projects anteriorly and medioventrally and is ventrally offset from the posterior margin of the otic capsule (fig. 28B). Distally, the descending process of the opisthotic is greatly expanded into a flat and subquadrangular surface, that contacts the posterior apex of the triangular and excavated floor of the fissura metotica (fig. 29A). Another process projects posteroventrally and laterally from the anteroventral margin of the crista interfenestralis, forming a recurved and mediolaterally expanded hooklike structure. This posteroventral process is completely preserved in the right side of the braincase and can be seen protruding laterally, just anterior and adjacent to the right fissura metotica (fig. 27A). The otic capsule (or cavum capsularis) is comprised of the prootic anteriorly and the opisthotic posteriorly, and it extends anteriorly and posteriorly around the fenestra ovalis. The otic capsule is relatively large and bulbous and expands medially to strongly constrict the mediolateral width of the braincase (fig. 28B). Anterior and dorsal to the otic capsule, the medial surface of the prootic is deeply depressed. Ventral to this depression, adjacent to the anterior edge of the otic capsule, there is a subcircular foramen that may represent the medial exit of the vestibulocochlear or auditory nerve (CN VIII; fig. 28B). Lateral to this foramen, there is an oblique cleft that, according to Galton (1985), might also transmit the auditory nerve, just dorsal to the dorsal border of the fenestra ovalis.

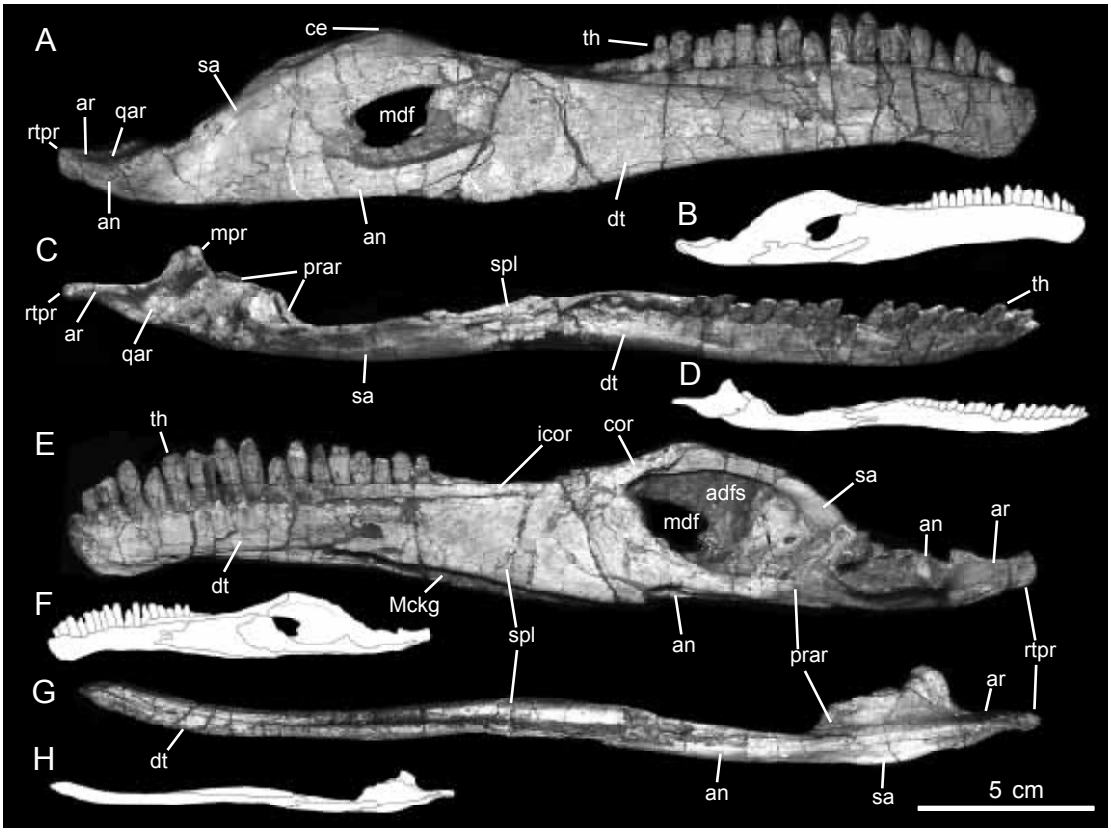

FIG. 31. Right mandible of *Plateosaurus erlenbergiensis* (AMNH FARB 6810). **A–B,** lateral; **C–D,** dorsal; **E–F,** medial; and **G–H,** ventral. Abbreviations in appendix 2.

Opisthotic-Exoccipital: Posterior to the prootic lies the fused opisthotic-exoccipital bones. The region of the opisthotic dorsal to the lateral wall of the prootic and lateral to the supraoccipital contains a large and deep elliptic excavation (fig. 27). Ventral to this excavation, the lateral surface of the opisthotic is medially recessed relative to the underlying lateral surface of the prootic. The lateroventral wall of the exoccipital, which articulates with the dorsolateral region of the basioccipital and contributes to the foramen magnum, contains two foramina for branches of the hypoglossal nerve (CN XII) (Galton, 1984). This observation is supported by the presence of a fine sutural line on the medial side of the posterior ventral wall of the braincase (which is composed of the opisthotic-exoccipital) that extends anteriorly from the laterodorsal corner of the occipital condyle (fig. 29A). The two hypoglossal foramina are found dorsal to that sutural line, ventral to which lies the basioccipital. The more posterior of this pair of foramina is relatively large and circular, and laterally conspicuous (fig. 27). The smaller foramen of the pair lies immediately anterior and ventral to the large one, behind the crista tuberalis (fig. 27B). The triangular surface on the anterior side of the crista tuberalis faces anterolaterally and dorsally. This surface is the floor of the fissura metotica and is excavated, becoming greatly expanded mediolaterally toward its anteroventral end.

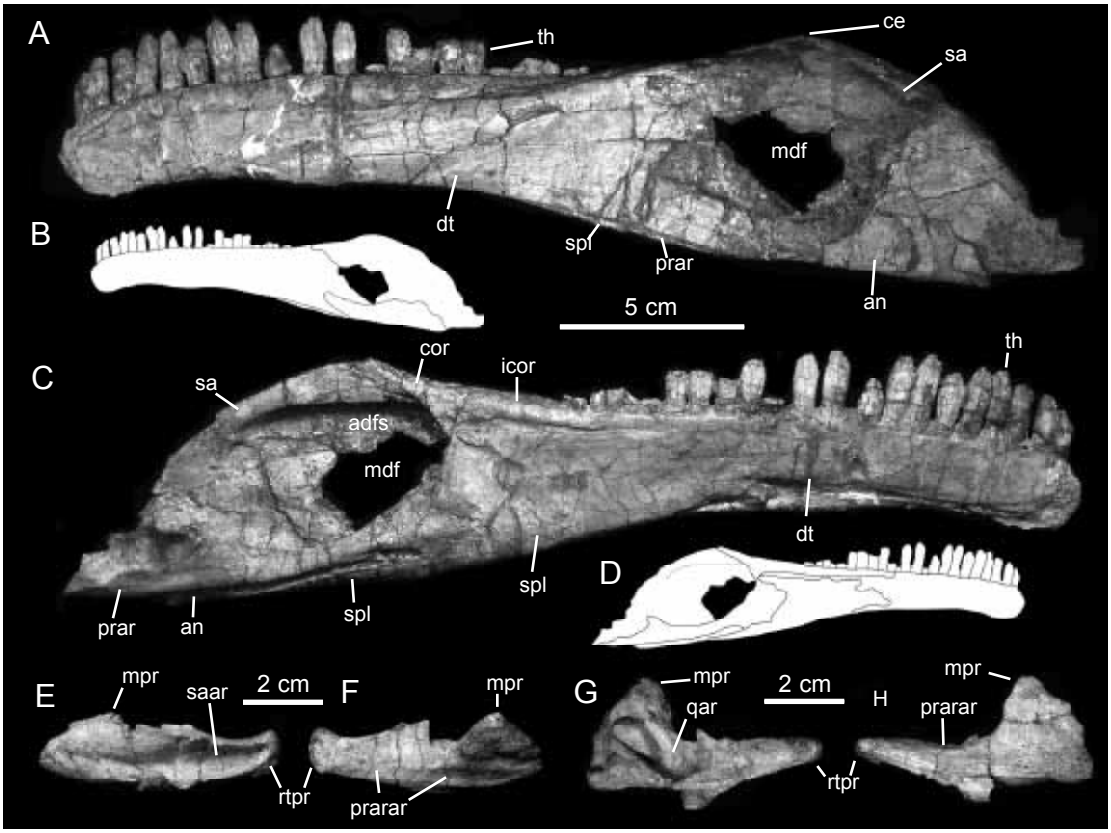

FIG. 32. Left mandible of *Plateosaurus erlenbergiensis* (AMNH FARB 6810). **A–B,** lateral; **C–D,** medial; **E,** lateral, **F,** medial, **G,** dorsal, and **H,** ventral views of left articular. Abbreviations in appendix 2.

Each paroccipital process extends posterior to the wedge-shaped end of the prootics. This long and large process projects posterodorsally and laterally, and is mediolaterally compressed (fig. 27). It is mediolaterally thicker at its proximal end, becoming gradually more compressed toward the distal end. Its dorsal and ventral margins diverge progressively from each other as the distal end of the process expands dorsoventrally. In dorsal view, the paroccipital process is gently arched, showing a gently concave medial side (fig. 28A). The long axes of both paroccipital processes form an angle of ~60°. Proximally, the dorsal surface of the opisthotic, between the base of the paroccipital process and the dorsolateral border of the foramen magnum formed by the supraoccipital, is deeply depressed (fig. 30B).

Supraoccipital: This element forms the dorsal half of the foramen magnum and the roof of the posterior region of the braincase (figs. 28A, 30B). In dorsal view, the supraoccipital is elongate and triangular, narrow anteriorly and widens gradually toward the dorsal margin of the foramen magnum. The dorsal surface of the supraoccipital is mediolaterally convex and displays a broad shallow longitudinal ridge. This ridge fits in between the left and right prootic anteriorly and the left and right opisthotic posteriorly. The dorsal surface of the supraoccipital slopes posteroventrally, forming a 125° angle relative to the surface

containing the foramen magnum. The supraoccipital contribution to the foramen magnum forms a semicircular arch with well-defined edges.

Mandible

As in other basal sauropodomorphs (Galton and Upchurch, 2004), the mandible of AMNH FARB 6810 is proportionally shallow, anteroposteriorly elongate and mediolaterally compressed (figs. 31, 32). The tooth-bearing dentary, is approximately three-fifths the length of the mandible. Posterior to the dentary, the lateral side of the mandible consists of the surangular dorsally and the angular ventrally; medially, the postdentary region of the mandible is composed of the coronoid and surangular dorsally, the prearticular ventrally, and the articular posteriorly (fig. 31E, F). The splenial articulates with the medial side of the posterior region of the dentary. On the lateral side of the mandible, just posterior to the dentary, there is a large mandibular fenestra, which extends along 8% the length of the mandible. It is oval in shape, longer anteroposteriorly than dorsoventrally, and bounded by the dentary anteriorly, the surangular dorsally, and the angular ventrally (fig. 31A, E). Dorsal and slightly posterior to the mandibular fenestra, the mandible reaches its maximum depth at the summit of a coronoid eminence where the mandible is about two and a half times deeper than at the anterior end of the dentary. The coronoid eminence is formed both by the coronoid and surangular. Ventrally, the anterior and posterior margins of the coronoid eminence meet at an angle of 145°. On the medial side of the mandible, just ventral to the coronoid eminence and posteromedial to the mandibular fenestra, lies a large adductor fossa (figs. 31E, 32C). This fossa is oval and longer anteroposteriorly than dorsoventrally. Its a long axis slightly oriented anterodorsally and is long as one-fifth of the entire mandibular length. The fossa is slightly larger in the left mandible of AMNH FARB 6810. The dorsal, anterior, and ventral margins of the adductor fossa have sharp, well-demarcated borders. In contrast, its posterior region is continuous with the medial surface of the surangular. There is a shallow foramen on the posteriormost region of the right mandible's adductor fossa (fig. 31E). This foramen is absent in the left mandible. The anterior half of the posterior region of the mandible is mediolaterally expanded and contains the glenoid fossa for articulation with the quadrate. The posterior end of the mandible is composed of a long retroarticular process that is about 10% of the length of the mandible. A Meckelian groove is present along the medioventral margin of the mandible, from the anterior region of the dentary to the area ventral to the prearticular (fig. 31E). This groove is exposed on the right mandible where it underlies the ventral margins of the prearticular posteriorly and the splenial and dentary anteriorly. It is enclosed, however, in the left mandible by the splenial.

Dentary: The dentary is an anteroposteriorly elongate and thick bony laminar element. The anterior half of the element shows a subrectangular profile laterally. Posterior to its midlength, the dentary becomes gradually deeper, so that its posterior margin is twice as deep as it is anteriorly. Posteriorly, the ventral margin of the dentary gradually diverges ventrally from the alveolar border of the tooth row (fig. 32A). In dorsal view, the dentary is slightly sinuous in profile (fig. 31C, G). The anterior fourth of the dentary curves ventrally about 10° relative to the ventral margin of the posterior and middle regions of the element. The symphysis is a coarse-textured

facet on the medial side of the anterior end of the dentary. The lateral surface of the dentary shows a large and obliquely oriented ridge; it slopes anteroventrally from the summit of the coronoid eminence to the ventral edge of the anterior third of dentary (figs. 31A, 32A). Associated with this ridge is the development of a lateroventrally inclined platform lateral to the posterior third of the tooth row (fig. 31C). There is a row of 10–12 small foramina on the lateral surface of the dentary, located at a short distance from the alveolar margin. Nearly all of these foramina are clustered within the anterior half of the tooth row and are widely spaced posteriorly.

There are 22 teeth in the dentary. The lingual surface of each tooth crown is coplanar with the medial surface of the dentary. The right dentary preserves the remains of five interdental plates between the first six teeth. These structures are subtriangular to subpentagonal in shape and rise from the alveolar margin between consecutive teeth. The left dentary shows two small fragments that may also represent interdental plates, between the fifth and sixth and the sixth and seventh teeth.

Surangular: This element forms most of the lateral wall of the posterior region of the mandible (fig. 31A). The surangular is mediolaterally compressed and anteroposteriorly elongate. Its dorsal margin is sigmoid, rising anterodorsally to form most of the coronoid eminence. Anterior to the coronoid eminence, the dorsal margin of the surangular slopes anteroventrally to form a wedge-shaped process that overlaps the posterodorsal end of the dentary and forms the dorsal border of the mandibular fenestra. The region of the surangular dorsal to the mandibular fenestra is dorsoventrally convex, so that the top surface faces dorsolaterally along the coronoid eminence. Ventral to this convexity, the lateral surface of the surangular is flat and overlapped ventrally by the angular. Posteriorly, the surangular becomes progressively shallower, wedging to an apex that overlaps the lateral side of the articular (fig. 31A, B). The lateral surface of this wedge is slightly concave and rugose in texture. A foramen is present posterodorsal to the surangular-angular articulation of the right mandible.

Most of the exposed medial surface of the surangular contains the adductor fossa. The coronoid bone overlaps the anterior end of that dorsomedial border of the surangular, at the anterodorsal region of the element (fig. 31E). Ventrally, on the medial side of the mandible, the surangular articulates with the prearticular, which ventrally bounds the adductor fossa. Posterior to the adductor fossa, the surangular appears to have fused with the articular but a suture between these two elements is not apparent.

Angular: The angular is an anteroposteriorly elongate osseous sheet. It forms the ventral third of the posterior region of the lateral side of the mandible, bounded by the dentary anteriorly and the surangular dorsally and posteriorly (figs. 31A, 32A). The angular consists of a fingerlike anterior process and a subtriangular posterior region. The anterior process projects anterodorsally onto the lateral surface of the posterior dentary. The posterior region of the angular shows a crenulated dorsal margin at the surangular articulation. The ventral margin of the angular is horizontal and folds medially, wrapping around the ventral margin of the mandible just below the adductor fossa and articulating medially with the ventral margin of the prearticular.

Splenial: The splenial is a thin lamina affixed to the medial wall of the dentary. It is roughly trapezoidal in shape, with an anteroposteriorly longer ventral margin (figs. 31E, 32C).

The anterior edge of the splenial has a very irregular profile (perhaps exaggerated by incomplete preservation) and anteroventrally slopes. The posterior margin of the splenial is crescent shaped and bifurcates into two processes. The longer posteroventral process projects posteriorly parallel to the ventral margin of the mandible, contacting the anteroventral ends of the angular and prearticular bones. The posterodorsal process of the surangular underlies the coronoid, contacting a short posteroventral expansion of the latter (fig. 31C).

Intercoronoid and Coronoid: The intercoronoid (or supradentary) is a bony strand that lies flush to the alveolar margin of the tooth row on the medial side of the mandible (figs. 31E, 32C). The ventral margin of the tapelike anterior two-thirds of the coronoid contacts the dentary and splenial. The anterior border of the intercoronoid articulates nearly seamlessly with the posterodorsally oriented, wedge-shaped region of the coronoid.

The coronoid is relatively small and elongate and borders the anterodorsal region of the adductor fossa while contacting the surangular (fig. 32C). The posterior third of the coronoid is dorsoventrally wide and bears a short, spurlike process that projects posteroventrally to contact the posterodorsal process of the splenial and the prearticular.

Prearticular: This element is anteroposteriorly elongate and irregularly shaped. The anterior half is mediolaterally compressed, gently arched, and dorsally concave (fig. 31E). Anteriorly it bifurcates to accommodate a short wedge-shaped process of the dentary. Medially, the anterior half of the prearticular articulates with the ventral region of the surangular and, ventrally, with the splenial and angular. The posterior half of the prearticular consists of a thin, ventrally and slightly medially directed lamina. The ventral surface of this lamina is mediolaterally concave while the dorsal side of the lamina forms the mediodorsal surface of a deep fossa, just anterior to the glenoid fossa. The posterior region of the posterior lamina of the prearticular underlies the articular.

Articular: The articular forms the posterior end of the mandible. The element is J-shaped in dorsal view and can be divided into two parts, an anterior region containing the glenoid fossa and the posteriormost retroarticular process (fig. 31C, E). The anterior region of the articular expands medially due to the presence of a pyramidal process that medially borders the glenoid fossa and shows three distinct concave facets. One of these facets faces ventrally and is overlapped by the posterior lamina of the prearticular. A second facet faces anteriorly and slightly laterally, and is ventrally continuous with the glenoid fossa. The third facet faces posteriorly and slightly dorsally, and is laterally continuous with the medial surface of the retroarticular process. The medial condyle of the quadrate rests on the latter facet. The glenoid fossa is oval and deep, and receives the lateral condyle of the quadrate and is bounded anteriorly by a ridge originating from the lateral margin of the articular. This ridge separates the glenoid fossa from an adjacent and more anteriorly located fossa bounded by the surangular and prearticular. Anteriorly, the articular does not show any distinctive articular boundary with the surangular.

The posterior two-thirds of the articular are composed of the retroarticular process. This process is mediolaterally compressed and triangular in cross section. Three surfaces can be distinguished facing laterally, medially, and dorsally. These surfaces are slightly concave and separated by sharp edges. The lateral surface contains a long and deep triangular depression

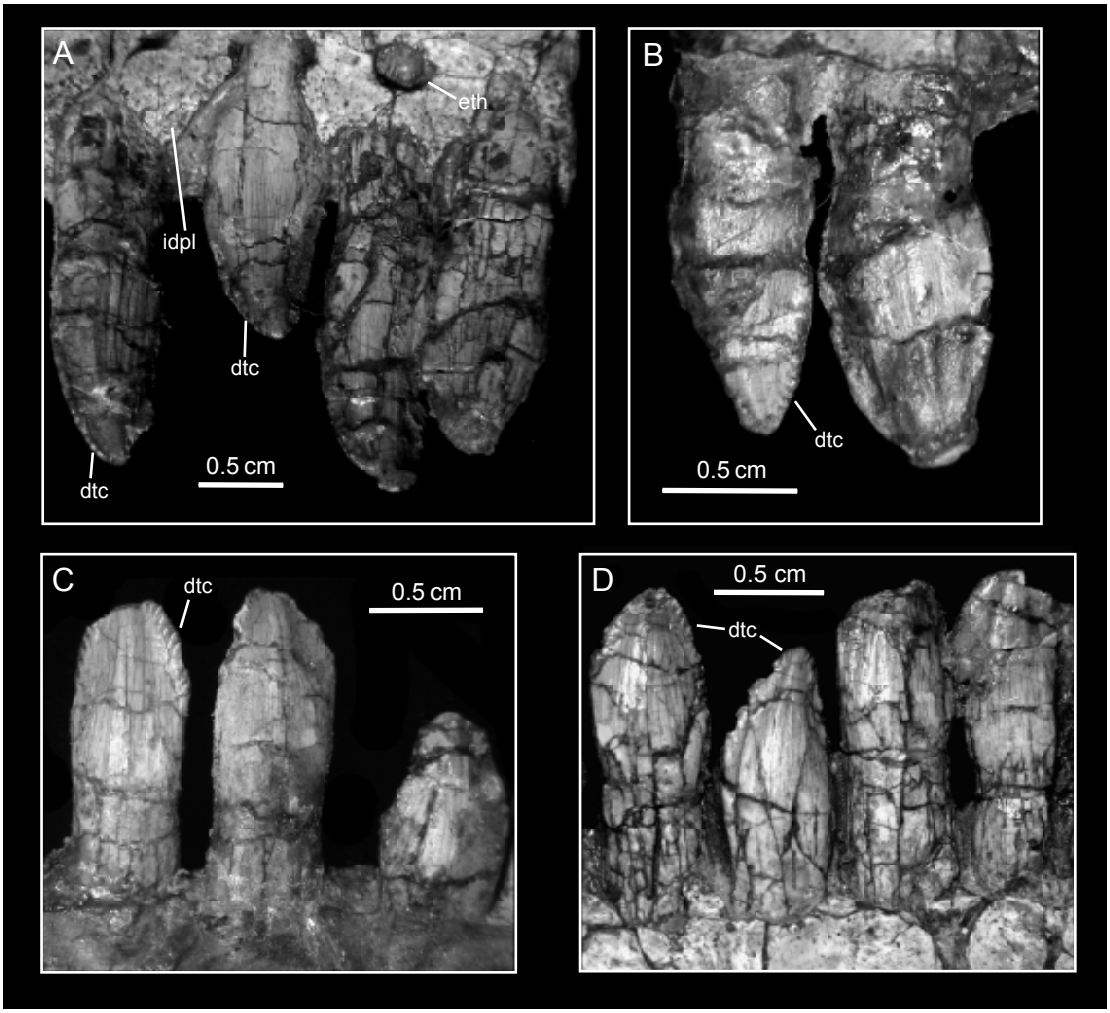

FIG. 33. Dentition of *Plateosaurus erlenbergiensis* (AMNH FARB 6810). **A,** right second through fifth premaxillary teeth in lingual view. **B,** left first and second maxillary tooth in labial view. **C,** left ninth trough eleventh dentary tooth in labial view. **D,** third through sixth right dentary tooth in lingual view. Abbreviations in appendix 2.

that accommodates the posterior wedge of the surangular. The retroarticular process becomes slightly shallower posteriorly and gradually more compressed mediolaterally, where it ends forming a rectangular margin seen in both lateral and medial views.

Dentition

In general, the tooth crowns are pencillike and labiolingually compressed, particularly near their apical margins (fig. 33). The height of tooth crowns is greater in the anterior region of the upper and lower tooth rows, decreasing gradually toward the posterior end of the maxilla and dentary. Thus, the height of the last tooth crown in the maxilla is less than half that of the ante-

riormost maxillary and all premaxillary teeth. The tooth crowns are slightly wider anteroposteriorly along the distal two-thirds of their total height. They are also slightly constricted anteroposteriorly proximal to their maximum width, at about midheight of the crown. The surface texture of the enamel is smooth; longitudinal lines can be seen in the enamel, but these are actually stained cracks (fig. 33). The mesial and distal carinae of tooth crowns converge distally to form an angle of approximately 75° at the apex. Marginal denticles are present, being subrectangular and elongate in shape (fig. 33C). The denticles do not cover, however, the entire mesial and distal margins of the crowns. They are found along the apical third or two-fifths of the crowns. The size of each individual denticle is approximately equal on the mesial and distal margins. The denticles are oriented obliquely relative to the long axis of the tooth. There are approximately one and a half to two denticles per millimeter of carina.

Premaxillary tooth crowns are slightly asymmetric in labial and lingual views: while the distal margin is vertical, the distal third of the mesial margin is curved, giving these teeth a bladelike appearance (fig. 33A). In mesial and distal views, these crowns are gently curved, so that the labial side is slightly convex and the lingual surface is slightly concave apicobasally. The labial and medial surfaces of the distal third of the crown are finely striated. The apices of two replacement crowns can be seen erupting directly dorsal and medial to the second and fourth right premaxillary teeth and are visible through small circular openings between consecutive interdental plates (fig. 33A).

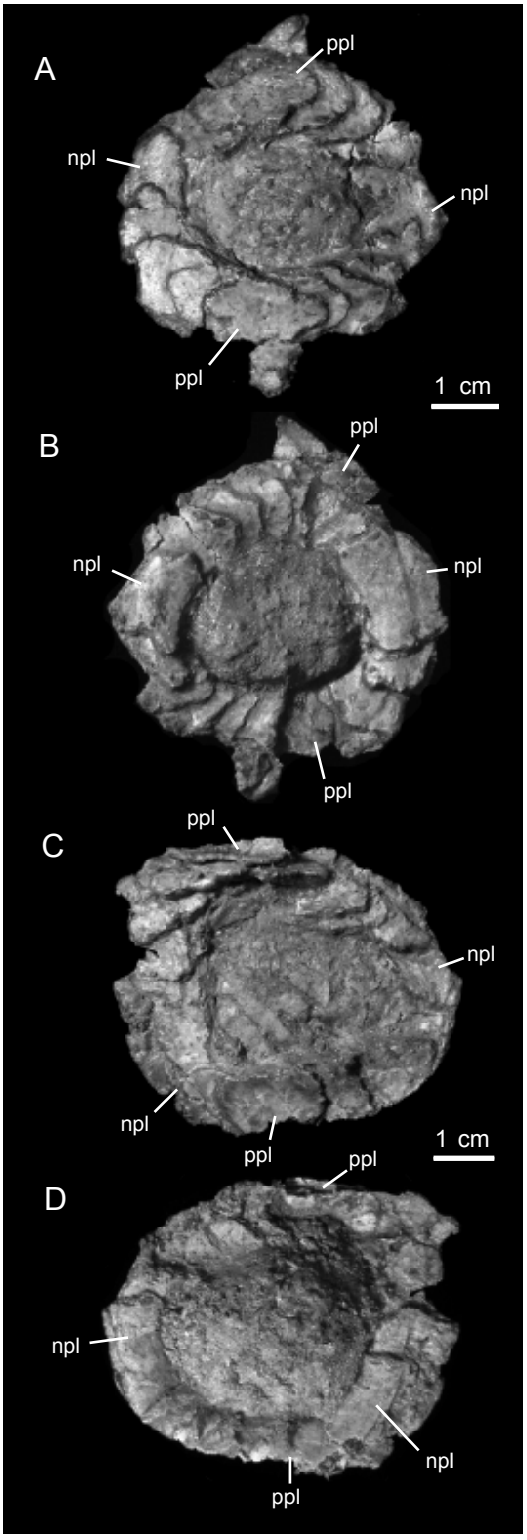

FIG. 34. Sclerotic rings of *Plateosaurus erlenbergiensis* (AMNH FARB 6810). **A,** lateral and **B,** medial views of right sclerotic ring. **C,** lateral and **D,** medial views of left sclerotic ring. Abbreviations in appendix 2.

The first four maxillary teeth show the same curvature and labial profile observed in the premaxillary ones. Distally, all the other tooth crowns have subparallel mesial and distal margins along the basal half of the crowns (fig. 33B). In the distal half of the maxillary tooth row, the long axes of tooth crowns are slightly oriented mesioventrally rather than vertically. As in the premaxilla, all maxillary tooth crowns have proximodistally concave lingual sides. This concavity is greater in the first five maxillary teeth, becoming less pronounced more distally in the tooth row. The lingual sides of the distal third of the crowns are flat. In contrast to those of the maxilla, the dentary teeth are vertically oriented (fig. 33C, D). Their lingual and labial surfaces are slightly convex mesiodistally, which results in a labiolingually compressed elliptical cross section. The distal thirds of dentary teeth are less expanded mesiodistally than those of maxillary teeth and the middle constriction is less evident.

Sclerotic Ring: This structure is preserved on both sides of the skull. It consists of a circular arrangement of 18 successively overlapping plates (fig. 34). Each plate is a subrectangular and very delicate bone lamina. In lateral view, and following the orientation of the sclerotic ring adopted by Galton (1984), a central dorsal and a central ventral plate overlaps each of the adjacent plates that lie anteriorly and posteriorly; these centered overlapping plates are the so-called positive plates (Lemmrich, 1931). Similarly and also in lateral view, an anterior and a posterior plate of the ring (the negative plates) are each dorsally and ventrally overlapped by adjacent plates (fig. 34A). Excluding the positive and negative plates, this configuration allows for the definition of four quadrants of sclerotic plates. Accordingly, the anterodorsal, anteroventral, posteroventral, and posterodorsal quadrants contain five, four, one, and four plates, respectively.

SYSTEMATIC PALEONTOLOGY

Dinosauria Owen, 1842
Saurischia Seeley, 1888
Sauropodomorpha Huene, 1932
Plateosaurus Meyer, 1837
P. erlenbergiensis Huene, 1905b

Synonymy: *P. longiceps* (Jaekel, 1913–1914).

Holotype: SMNS 6014, consisting of a partial skull and part of the skeleton including several vertebrae, partial pectoral girdle and forelimb, partial ilium, ischium, and most of the hindlimb elements (Galton, 2001).

Referred material: Hundreds of disarticulated elements, as well as complete skeletons including at least 10 skulls (Galton and Upchurch, 2004), including AMNH FARB 6810.

Occurrence: Various Middle-Late Norian (Late Triassic) formations, including the Trossingen (Baden-Württemberg, Germany), Knollenmergel (Niedersachsen and Sachsen-Anhalt, Germany), Obere Bunte Mergel (Aargau, Switzerland), Marnes Irisées Supérieures (Jura and Doubs, France), and Fleming Fjord (eastern Greenland) Formations (Galton and Upchurch, 2004).

Emended diagnosis: Occipital condyle above level of parasphenoid; basisphenoid with transverse, subvertical lamina extending between basipterygoid processes, with ventrally projecting median process; dorsal end of lacrimal with broad and weakly rugose lateral sheet that covers posterodorsal corner of antorbital fenestra; peglike process projected medially from middle of palatine; and nasal length greater than half the length of skull roof (after Galton [1990; 2001], Yates [2003b], and Galton and Upchurch [2004]).

Comments: Galton (2001) regarded *Plateosaurus erlenbergiensis* Huene, 1905b, as a nomen dubium because of the poor and incomplete preservation of the type skull and postcranial skeleton. However, this specimen (SMNS 6014) contains sufficient anatomical information to be diagnostic. In particular, it displays three of the autapomorphies proposed here to diagnose *P. erlenbergiensis*: occipital condyle above the level of the parasphenoid; basisphenoid with transverse, subvertical lamina extending between the basipterygoid processes, with ventrally projecting median process; and a peglike process projected medially from the middle of the palatine. Therefore, and regardless of the quality of its preservation or extent of anatomical completeness, SMNS 6014 forms an adequate and diagnosable type specimen.

At least two of the autapomorphies of *Plateosaurus erlenbergiensis* (i.e., the peglike process of the palatine and the presence of subvertical lamina between the basipterygoid processes of the basisphenoid) have previously been proposed as derived characters of *P. longiceps* (Galton, 2001; Galton and Upchurch, 2004). Since *P. erlenbergiensis* Huene, 1905b, clearly has priority over *P. longiceps* Jaekel, 1913–1914, we regard the latter as a junior synonym of *P. erlenbergiensis*.

DISCUSSION AND CONCLUSION

The taxonomy of *Plateosaurus* has undergone numerous changes since early work on this taxon. The number of constituent species has been drastically reduced from the numerous taxa erected by early authors (Meyer, 1837; Rutimeyer, 1856; Pidancet and Chopard, 1862; Fraas, 1894, 1913, 1915; Huene, 1905a, 1905b, 1908, 1932; Jaekel, 1911, 1913–1914) to the one (Galton, 1984, 1985, 1990; Weishampel and Westphal, 1986; Weishampel and Chapman, 1990; Moser, 2000, 2003), or two (Galton, 2001; Yates, 2003b; Galton and Upchurch, 2004) species recognized in more recent studies. Among the latter, there has been little consensus as to which species is to be considered valid. For example, Galton (2001) and Galton and Upchurch (2004) recognized *P. engelhardti* and *P. longiceps* as the two valid species, whereas Yates (2003b) only regarded *P. engelhardti* and a possible metaspecies, *P. gracilis*, as valid.

Even though it is one of the best known specimens, the taxonomic placement of AMNH FARB 6810 has been nearly as contentious as the taxonomic composition of *Plateosaurus*: the specimen has been variably referred to *Plateosaurus engelhardti* (e.g., Galton 1984, 1985, 1986, 1990; Pol and Powell, 2007; Mallison, 2010a, 2010b) or to *P. longiceps* (Galton, 2001; Galton and Upchurch, 2004; Sereno, 2007).

All the autapomorphies of *Plateosaurus longiceps* provided by Galton (2001) and Galton and Upchurch (2004) can be observed in AMNH FARB 6810. These are: nasal length greater

than half the length of the skull roof; medially directed, peglike process from the middle of the palatine; and transverse subvertical lamina of the basisphenoid between the basipterygoid processes, with median ventrally directed process. Pending a detailed analysis of the morphological variation in the available cranial and postcranial materials of the genus *Plateosaurus* that would clarify the lack of consensus currently present in the literature regarding the taxonomic composition of this genus, we tentatively refer AMNH 6810 to *P. erlenbergiensis*. This decision is based on the presence in AMNH 6810 of all the autapomorphies of *P. erlenbergiensis* (see above), including those observable in the holotype of this species.

ACKNOWLEDGEMENTS

We thank the American Museum of Natural History for funding this study through a Kalbfleisch Research Fellowship. Mick Ellison is thanked for scanning the historical materials. Barbara Mathe and Tom Baione provided access to historical photographs. We are grateful to the advice provided by Adam M. Yates and Diego Pol on various aspects of the anatomy and systematics of *Plateosaurus*. Thanks to Alana Gishlick for helping with archival material. Additional support for this study was also provided by the Division of Paleontology AMNH and NSF DEB 0958972.

REFERENCES

Attridge, J., A.W. Crompton, F.A. Jenkins, Jr. 1985. The southern African Liassic prosauropod *Massospondylus* discovered in North America. Journal of Vertebrate Paleontology 5: 128–132.

Bai, Z., J. Yang, and G. Wang. 1990. *Yimenosaurus*, a new genus of Prosauropoda from Yimen County, Yunnan province. Yuxiwenebo (Yuxi Culture and Scholarship) 1: 14–23.

Barrett, P.M. 2004. Sauropodomorph dinosaur diversity in the upper Elliot Formation (*Massospondylus* range zone: Lower Jurassic) of South Africa. South African Journal of Science 100: 501–503.

Barrett, P.M. 2009. A new basal sauropodomorph dinosaur from the Upper Elliot Formation (Lower Jurassic) of South Africa. Journal of Vertebrate Paleontology 29: 1032–1045.

Barrett, P.M., P. Upchurch, and W. Xiao-Lin. 2005. Cranial osteology of *Lufengosaurus huenei* Young (Dinosauria: Prosauropoda) from the Lower Jurassic of Yunnan, People's Republic of China. Journal of Vertebrate Paleontology 25: 806–822.

Barrett, P.M., P. Upchurch, X.-D. Zhou, and X.-L. Wang. 2007. The skull of *Yunnanosaurus huangi* Young, 1942 (Dinosauria: Prosauropoda) from the Lower Lufeng Formation (Lower Jurassic) of Yunnan, China. Biological Journal of the Linnean Society 150: 319–341.

Benton, M.J., L. Juul, G.W. Storrs, and P.M. Galton. 2000. Anatomy and systematics of the prosauropod dinosaur *Thecodontosaurus antiquus* from the Upper Triassic of southwest England. Journal of Vertebrate Paleontology 20: 77–108.

Bonaparte, J.F. 1969. Comments on early saurischians. Zoological Journal of the Linnean Society 48: 471–480.

Bonaparte, J.F. 1978. *Coloradia brevis* n. g. et n. sp. (Saurischia: Prosauropoda), dinosaurio Plateosauridae de la Formación Los Colorados, Triásico superior de La Rioja, Argentina. Ameghiniana 15: 327–332.

Bonaparte, J.F. 1999. Evolución de las vertebras presacras en Sauropodomorpha. Ameghiniana 36: 115–187.

Bonaparte, J.F., and J.A. Pumares. 1995. Notas sobre el primer cráneo de *Riojasaurus incertus* (Dinosauria, Prosauropoda, Melanorosauridae) del Triásico Superior de la Rioja, Argentina. Ameghiniana 32: 341–349.

Charig, A.J., J. Attridge, and A.W. Crompton. 1965. On the origin of the sauropods and the classification of the Saurischia. Proceedings of the Linnean Society of London 176: 197–221.

Colbert, E.H. 1964. Relationships of the saurischian dinosaurs. American Museum Novitates 2181: 1–24.

Cruickshank, A.R. 1975. The origin of sauropod dinosaurs. South African Journal of Science 71: 89–90.

Fraas, E. 1894. *Zanclodon bavaricus*. *Neues* Jahrbuch für Mineralogie, Geologie und Paläontologie 1: 203–204.

Fraas, E. 1913. Die neuesten Dinosaurierfunde in der Schwäbischen Trias. Naturwissenschaften 45: 1097–1100.

Fraas, E. 1915. *Plateosaurus integer*. *Neues* Jahrbuch für Mineralogie, Geologie und Paläontologie 1915: 3.

Galton, P.M. 1973. On the anatomy and relationships of *Efraasia diagnostica* (Huene) n. gen., a prosauropod dinosaur (Reptilia: Saurischia) from the Upper Triassic of Germany. Paläontologische Zeitschrift 47: 229–255.

Galton, P.M. 1976. Prosauropod dinosaurs (Reptilia: Saurischia) or North America. Postilla 169: 1–98.

Galton, P.M. 1984. Cranial anatomy of the prosauropod dinosaur *Plateosaurus* from the Knollenmergel (Middle Keuper, Upper Triassic) of Germany. Geologica et Palaeontologica 18: 139–171.

Galton, P.M. 1985. Cranial anatomy of the prosauropod dinosaur *Plateosaurus* from the Knollenmergel (Middle Keuper, Upper Triassic) of Germany. II. All the cranial material and details of soft-part anatomy. Geologica et Palaeontologica 19: 119–159.

Galton, P.M. 1986. Prosauropod dinosaur *Plateosaurus* (= *Gresslyosaurus*) (Saurischia: Sauropodomorpha) from the Upper Triassic of Switzerland. Geologica et Palaeontologica 20: 167–183.

Galton, P.M. 1990. Basal Sauropodomorpha – Prosauropoda. *In* D.B. Weishampel, P. Dodson, and H. Osmólska (editors), The Dinosauria: 320–344. Berkeley: University of California Press.

Galton, P.M. 1997. Comments on sexual dimorphism in the prosauropod *Plateosaurus engelhardti* (Upper Triassic, Trossingen). Neues Jahrbuch für Geologie und Paläontologie Mh 1997: 674–682.

Galton, P.M. 2000. The prosauropod dinosaur *Plateosaurus* Meyer, 1837 (Saurischia: Sauropodomorpha). I. The syntypes of *P. engelhardti* Meyer, 1837 (Upper Triassic, Germany), with notes on other European prosauropods with "distally straight" femora. Neues Jahrbuch für Geologie und Paläontologie Abhandlungen 216: 233–275.

Galton, P.M. 2001. The prosauropod dinosaur *Plateosaurus* Meyer, 1837 (Saurischia; Sauropodomorpha; Upper Triassic). II. Notes on the referred species. Revue de Paléobiologie 20: 435–502.

Galton, P.M., and D. Kermack. 2010. The anatomy of Pantydraco caducus, a very basal sauropodomorph dinosaur from the Rhaetian (Upper Triassic) of South Wales, UK. Revue de Paléobiologie 29: 341–404.

Galton, P.M., and P. Upchurch. 2004. Prosauropoda. *In* D.B. Weishampel, P. Dodson, and H. Osmólska (editors), The Dinosauria, 2nd ed.: 232–258. Berkeley: University of California Press.

Galton, P.M., A.M. Yates and D. Kermack. 2007. Pantydraco n. gen. for Thecodontosaurus caducus Yates, 2003, a basal sauropodomorph dinosaur from the Upper Triassic or Lower Jurassic of South Wales, UK. Neues Jahrbuch für Geologie und Paläontologie Abhandlungen 243: 119–125.

Gauffre, F.-X. 1995. Phylogeny of prosauropod dinosaurs. Journal of Vertebrate Paleontology 15: 31A.

Gow, C.E., J.W. Kitching, and M.A. Raath. 1990. Skulls of the prosauropod dinosaur *Massospondylus carinatus* Owen in the collections of the Bernard Price Institute for Palaeontological Research. Palaeontologia Africana 27: 45–58.

Gunga, H.-C., T. Suthau, A. Bellmann, A. Friedrich, T. Schwanebeck, S. Stoinski, T. Trippel, K. Kirsch, and O. Hellwich. 2007. Body mass estimations for *Plateosaurus engelhardti* using laser scanning and 3D reconstruction methods. Naturwissenschaften 94: 632–630.

Huene, F. von. 1905a. Über die Nomenklatur von *Zanclodon*. Zentralblatt für Mineralogie, Geologie und Paläontologie 1905: 10–12.

Huene, F. von. 1905b. Über die Trias-Dinosaurier Europas. Zeitschrift der Deutschen Geologischen Gesellschaft 57: 345–349.

Huene, F. von. 1908. Die Dinosaurier der europäischen Triansformationen mit Berücksichtigung der aussereuropäischen Vorkommnisse. Geologische und Paläontologische Abhandlungen Supplement 1: 1–419.

Huene, F. von. 1926. Vollständige Osteologie eines Plateosauriden aus dem schwäbischen Keuper. Geologische und Paläontologische Abhandlungen 15: 129–179.

Huene, F. von. 1932. Die fossile Reptil-Ordnung Saurischia, ihre Entwicklung und Geschichte. Monographien zur Geologie und Paläontologie 4: 1–361.

Jaekel, O. 1911. Die Wirbeltiere. Eine Übersicht über die fossilen und lebenden Formen. Berlin: Borntraeger.

Jaekel, O. 1913–1914. Über die Wirbeltierfunde in der oberen Trias von Halberstadt. Paläontologische Zeitschrift 1: 155–215.

Jenkins, F.A., Jr., et al. 1995. Late Triassic continental vertebrates and depositional environments of the Fleming Fjord Formation, Jameson Land, east Greenland. Meddelelser om Grønland Geoscience 32: 3–25.

Klein, N. 2004. Bone histology and growth of the prosauropod dinosaur *Plateosaurus engelhardti* Meyer, 1837 from the Norian bonebeds of Trossingen (Germany) and Frick (Switzerland). Ph.D. dissertation, University of Bonn, 128 pp.

Leal, L.A., S.A.K. Azevedo, A.W.A. Kellner, and A.A.S. Da Rosa. 2004. A new early dinosaur (Sauropodomorpha) from the Caturrita Formation (Late Triassic), Paraná Basin, Brazil. Zootaxa 690: 1–24.

Mallison, H. 2010a. The digital *Plateosaurus* I: body mass, mass distribution and posture assessed using CAD and CAE on a digitally mounted complete skeleton. Palaeontologia Electronica 13: 1–26.

Mallison, H. 2010b. The digital *Plateosaurus* II: An assessment of the range of motion of the limbs and vertebral column and of previous reconstructions using a digital skeletal mount. Acta Palaeontologica Polonica 55: 433–458.

Martínez, R.N. 1999. The first South American record of *Massospondylus* (Dinosauria: Sauropodomorpha). Journal of Vertebrate Paleontology 19: 61A.

Martínez, R.N. 2009. *Adeopapposaurus mognai*, gen. et sp. nov. (Dinosauria: Sauropodomorpha), with comments on adaptations of basal Sauropodomorpha. Journal of Vertebrate Paleontology 29: 142–164.

Martínez, R.N., and O.A. Alcober. 2009. A basal sauropodomorph (Dinosauria: Saurischia) from the Ischigualasto Formation (Triassic, Carnian) and the early evolution of Sauropodomorpha. PLoS ONE 4: 1–12.

Meyer, H. von. 1837. Briefliche Mitteilung an Prof. Bronn über *Plateosaurus engelhardti*. Neues Jahrbuch für Mineralogie, Geognosie, Geologie und Petrefakten-Kunde 1837: 316.

Moser, M. 2000. The influence of pedogenesis on the taxonomy of *Plateosaurus*. *In* E. Frey (editor), 5th European Workshop on Vertebrate Paleontology. Program. Abstracts. Excursion Guides: 57. Karlsruhe: Staatliches Museum fur Naturkunde.

Moser, M. 2003. *Plateosaurus engelhardti* Meyer, 1837 (Dinosauria: Sauropodomorpha) aus dem Feuerletten (Mittelkeuper, Obertrias) von Bayern. Zitteliana B 24: 188.

Novas, F.E., M.D. Ezcurra, S. Chatterjee, and T.S. Kutty. 2011. New dinosaur species from the Upper Triassic Upper Maleri and Lower Dharmaram formations of Central India. Earth and Environmental Science Transactions of the Royal Society of Edinburgh 101; 303–349.

Pidancet, J., and S. Chopard. 1862. Note sur un saurian gigantesque aux Marnes irisées. Comptes Rendús de l'Academie des Sciences de Paris 54: 1259–1262.

Pol, D., and J.E. Powell. 2007. Skull anatomy of *Mussaurus patagonicus* (Dinosauria: Sauropodomorpha) from the Late Triassic of Patagonia. Historical Biology 19: 125–144.

Pol, D., A. Garrido, and I.A. Cerda. 2011. A new sauropodomorph dinosaur from the Early Jurassic of Patagonia and the origin and evolution of the sauropod-type sacrum. PLoS ONE 6 (1): e14572. [doi: 10.1371/journal.pone.0014572]

Romer, A.S. 1956. Osteology of the reptiles. Chicago: University of Chicago Press.

Rutimeyer, L. 1856. Reptilienknochen aus dem Keuper. Allgemeine schweizerische Gesellschaft für die gesammten Naturwissenschaften Verhandlungen 41: 62–64.

Sander, P.M. 1992. The Norian *Plateosaurus* bonebeds of central Europe and their taphonomy. Palaeogeography, Palaeoclimatology, Palaeoecology 93: 255–299.

Sander, P.M., and N. Klein. 2005. Developmental plasticity in the life history of a prosauropod dinosaur. Science 310: 1800–1802.

Sereno, P.C. 1989. Sauropod monophyly and basal sauropodomorph phylogeny. Journal of Vertebrate Paleontology 9: 38A.

Sereno, P.C. 1999. The evolution of dinosaurs. Science 284: 2137–2147.

Sereno, P.C. 2007. Basal Sauropodomorpha: historical and recent phylogenetic hypotheses, with comments on *Ammosaurus major* (Marsh, 1889). Special Papers in Palaeontology 77: 261–289.

Sertich, J.J.W., and M.A. Loewen. 2010. A new basal sauropodomorph dinosaur from the Lower Jurassic Navajo Sandstone of southern Utah. PLoS ONE 5: 1–17. [doi:10.1371/journal.pone.0009789]

Smith, N.D., and D. Pol. 2007. Anatomy of a basal sauropodomorph dinosaur from the Early Jurassic Hanson Formation of Antarctica. Acta Palaeontologica Polonica 52: 657–674.

Sues, H.D., R.R. Reisz, S. Hinic, and M.A. Raath. 2004. On the skull of *Massospondylus carinatus* Owen, 1854 (Dinosauria: Sauropodomorpha) from the Elliot and Clarens formations (Lower Jurassic) of South Africa. Annals of the Carnegie Museum 73: 239–257.

Upchurch, P., P.M. Barrett, and P.M. Galton. 2007. A phylogenetic analysis of basal sauropodomorph relationships: implications for the origin of sauropod dinosaurs. Special Papers in Palaeontology 77: 57–90.

Weishampel, D.B., and R.E. Chapman. 1990. Morphometric study of *Plateosaurus* from Trossingen (Baden-Württemberg, Federal Republic of Germany). *In* K. Carpenter and P. J Currie (editors), Dinosaur systematics: perspectives and approaches: 43–51. Cambridge: Cambridge University Press.

Weishampel, D.B., and F. Westphal. 1986. Die Plateosaurier von Trossingen im Geologischen Institut der Eberhard-Karls-Universität Tübingen. Ausstellungskataloge der Universität Tübingen 19: 1–27.

Wilson, J.A., and K.A. Curry Rogers. 2005. Introduction: monoliths of the Mesozoic. *In* K.A. Curry Rogers and J.A. Wilson (editors), The sauropods: evolution and paleobiology: 1–15. Berkeley: University of California Press.

Wilson, J.A., and P.C. Sereno. 1998. Early evolution and higher-level phylogeny of sauropod dinosaurs. Memoir of the Society of Vertebrate Paleontology 5: 1–68.

Witmer, L.M. 1997. The evolution of the antorbital cavity in archosaurs: a study in soft-tissue reconstruction in the fossil record with analysis of the function of pneumacity. Memoir of the Society of Vertebrate Paleontology 3: 1–75.

Yates, A.M. 2003a. A new species of the primitive dinosaur *Thecodontosaurus* (Saurischia: Sauropodomorpha) and its implications for the systematics of early dinosaurs. Journal of Systematic Palaeontology 1: 1–42.

Yates, A.M. 2003b. The species taxonomy of the sauropodomorph dinosaurs from the Löwenstein Formation (Norian, Late Triassic) of Germany. Palaeontology 46: 317–337.

Yates, A.M. 2004. *Anchisaurus polyzelus* (Hitchcock): the smallest known sauropod dinosaur and the evolution of gigantism among sauropodomorph dinosaurs. Postilla 230: 1–57.

Yates, A.M. 2007. The first complete skull of the Triassic dinosaur *Melanorosaurus* Huaughton (Sauropodomorpha: Anchisauria). *In* P.M. Barrett and D.J. Batten (editors), Evolution and palaeobiology of early sauropodomorph dinosaurs. Special Papers in Palaeontology 77: 9–55. London: Willey-Blackwell.

Yates, A.M. 2010. A revision of the problematic sauropodomorph dinosaurs from Manchester, Connecticut and the status of *Anchisaurus* Marsh. Palaeontology 53: 739–752.

Yates, A.M. ,and J.W. Kitching. 2003. The earliest known sauropod dinosaur and the first steps towards sauropod locomotion. Proceedings of the Royal Society of London Series B Biological Sciences 270: 1753–1758.

Yates, A.M., M.F. Bonnan, J. Neveling, A. Chinsamy, and M.G. Blackbeard. 2010. A new transitional sauropodomorph dinosaur from the Early Jurassic of South Africa and the evolution of sauropod feeding and quadrupedalism. Proceedings of the Royal Society Series B Biological Sciences 277: 787–794.

Young, C.-C. 1941a. A complete osteology of *Lufengosaurus huenei* Young (gen. et sp. nov.) from Lufeng, Yunnan, China. Palaeontologia Sinica Series C 7: 1–53.

Young, C.-C. 1941b. *Gyposaurus sinensis* (sp. nov.), a new Prosauropoda from the Upper Triassic Beds at Lufeng, Yunnan. Bulletin of the Geological Society of China 21: 205–253.

Young, C.-C. 1942. *Yunnanosaurus huangi* Young (gen. et sp. nov.), a new Prosauropoda from the Red Beds at Lufeng, Yunnan. Bulletin of the Geological Society of China 22: 63–104.

Zhang ,Y.-H., and Yang Z.-L. 1994. A complete osteology of the Prosauropoda in the Lufeng Basin, Yunnan, China. *Jingshanosaurus*. Kunming: Yunnan Science and Technology Publishing House.

APPENDIX 1

Institutional Abbreviations

AMNH FARB	American Museum of Natural History (Fossil Amphibian, Reptile, and Bird collection), New York
BSP	Bayerische Staatssammlung für Paläontologie und Historische Geologie, Munich, Germany
GPIT	Institut und Museum für Geologie und Paläontologie der Universität Tübingen, Tübingen, Germany
HMN	Humboldt Museum für Naturkunde, Berlin, Germany
MB	Museum für Naturkunde, Berlin, Germany
SMNS	Staatliches Museum für Naturkunde, Stuttgart, Germany
UE	Unniversität Erlangen, Institut für Geologie und Mineralogie, Erlangen, Germany

APPENDIX 2

Anatomical Abbreviations

adfs	adductor fossa
adrg	anterodorsal ridge
afg	anterior flange
aitf	anterior margin of infratemporal fenestra
aitm	anterior infratemporal margin
alfg	anterolateral flange
alstf	anterolateral margin of supratemporal fenestra
ampr	anteromedial process
an	angular
aof	antorbital fenestra
aofs	antorbital fossa
aom	anterior orbital margin
ar	articular
arm	anterior ramus
bo	basioccipital
bpar	articular depression for basipterygoid process of basisphenoid
bpf	basipterygoid flange
bs	basisphenoid
bsar	articular surface for basisphenoid
bspr	basisphenoid process
bstpr	basipterygoid process
cdl	lateral condyle
cdm	medial condyle
ce	coronoid eminence
ci	crista interfenestralis
coc	coracoid
cor	coronoid
cp	crista prootica
crb	cerebral cavity
ct	crista tuberalis
dp	descending process of the opisthotic
dpqrm	dorsal process of quadrate ramus
dpr	dorsal process
dpx	posterior apex of dorsal process
dsll	dorsum sellae
dt	dentary
dtc	denticles
epptg	epipterygoid
epptgpr	epipterygoid process
eptar	articular surface for epipterygoid

eptgar	articular margin or surface for ectopterygoid
eth	erupting tooth
excc	exoccipital
excpr	exoccipital process
f	frontal
far	articular socket and margin for frontal
fm	foramen magnum
fo	fenestra ovalis (= fenestra vestibuli)
fom	foramen magnum
fos	fossa
fpr	frontal process
fsm	fissura metotica
hm	humerus
ic	passage of internal carotid artery
icor	intercoronoid
idpl	interdental plate
itf	margin of infratemporal fenestra
j	jugal
jar	articular groove or surface for jugal
jfg	jugal flange
jpr	jugal process
jrm	jugal ramus
lc	lacrimal
lcar	articular surface for lacrimal
lcd	opening of the lacrimal duct
lcfg	lacrimal flange
lcpr	lacrimal process
lcjrg	lacrimo-jugal ridge
lfg	lateral flange
ls	laterosphenoid
lsar	articular surface for laterosphenoid
lt	left
Mckg	Meckelian groove
mdf	mandibular fenestra
mfg	medial flange
mnpr	median process
mp	attachment surtace for muscle protractor pterygoideus
mpr	medial process of basisphenoid
mrg	median ridge
mt	rock matrix
mtx	rock matrix (cast)
mx	maxilla
mxar	articular margin or surface for maxilla
mxare	edge for contact with maxilla
mxpr	maxillary process
mxrm	maxillary ramus
nf	narial fenestra
nfam	anterior marin of narial fenestra
npl	negative plate
nr	narial recess (narial fossa)
ns	nasal
nsar	articular surface for nasal
nspr	nasal process
obm	orbital margin
obt	orbital cavity
occ	occipital condyle
opar	articular surface for opisthotic
oppr	opisthotic process
opth	opisthotic
osar	articular surface for orbitosphenoid
otc	otic capsule (cavum capsularis)
pal	palatine
palfg	palatine flange
paof	posterior margin of anterorbital fenestra
par	parietal
parar	articular surface for parietal
parpr	parietal process
pas	parasphenoid
pdpr	posterodorsal process
peg	peglike process
pf	prefrontal
pfar	articular surface for prefrontal
pitf	posterior margin of infratemporal fenestra
plfg	posterolateral flange
pmx	premaxilla
pmnf	posterior margin of narial fenestra
pmxar	articular surface for premaxilla
pmxpr	premaxillary process
po	postorbital

poar	articular surface for postorbital
pobpr	postorbital process
pocpr	paroccipital process
pom	posterior orbital margin
popr	posterior process
porm	postorbital ramus
ppl	positive plate
ppx	posterior apex of maxillary ventral ramus
prar	prearticular
prarar	articulation surface for prearticular
proo	prootic
prooar	articular surface for prootic
proopr	prootic process
pstf	posterior margin of supratemporal fenestra
ptg	pterygoid
ptgar	articular surface for pterygoid
ptgfg	pterygoid flange
pvp	anterior posteroventral process of the crista interfenestralis
pvpr	posteroventral process
q	quadrate
qar	articular surface for quadrate
qct	quadrate cotylus
qh	quadrate head
qj	quadratojugal
qjar	articular margin for quadratojugal
qjnt	articular notch for quadratojugal
qjrm	quadratojugal ramus
qpr	quadrate process
qrm	quadrate ramus
rd	radius
rib	rib(s)
rmlm	recessed medial lamina of dorsal process
rt	right
rtpr	retroarticular process
sa	surangular
saar	articular sulcus for surangular
scp	scapula
sk	skull
sllt	sella turcita
so	supraoccipital
soar	articular surface for supraoccipital
sphtb	sphenooccipital tubercles (= basal tubera)
spl	splenial
sq	squamosal
sqar	articular surface for squamosal
sqrm	squamosal ramus
stf	supratemporal fenestra
stp	stapes
th	tooth
ul	ulna
vc	exit of vidian canal
vfg	ventral flange
vmfg	vomeral flange
vml	left vomer
vmr	right vomer
vpqrm	ventral process of quadrate ramus
vpr	ventral process
II	foramen for optic nerve
IV	foramen for trochlear nerve
V	foramen prooticum (for trigeminal nerve)
V_2	foramen for maxillary ramus of trigeminal nerve
V_3	foramen for mandibular ramus of trigeminal nerve
VI	foramen for abducens nerve
VII	foramen for facial nerve
VII_p	foramen for palatine ramus of facial nerve
VIII	foramen for vestibulocochlear (auditory) nerve
IX	foramen for glossopharyngeal nerve
X	foramen for vagus nerve
XI	foramen for spinal accessory nerve
XII	foramen for hypoglossal nerve

Complete lists of all issues of *Novitates* and *Bulletin* are available on the web (http://digitallibrary.amnh.org/dspace). Order printed copies on the web from http://www.amnhshop.com or via standard mail from:

American Museum of Natural History—Scientific Publications
Central Park West at 79th Street
New York, NY 10024

♾ This paper meets the requirements of ANSI/NISO Z39.48-1992 (permanence of paper).